

Chapter 10

The Physics of Tunable Disorder in Semiconductor Alloys

Angelo Mascarenhas and Yong Zhang

National Renewable Energy Laboratory, Golden, Colorado, U.S.A.

Key words: ordering, alloy statistics, band structure, optical anisotropy, band offset, GaInP

Abstract: A review of the key changes in electronic properties that result from spontaneous ordering in III-V semiconductor alloy is presented. The intrinsic as well as extrinsic effects of the phenomenon are reviewed. The band structure changes and resulting optical anisotropy, the order parameter and the effects of controllable alloy statistical fluctuations on optical properties, orientational domain boundaries and the formation of orientational superlattices, the band-offsets between ordered GaInP and GaAs, and the effects of microstructural features such as anti-phase boundary defects on optical spectra are discussed. Wherever applicable, both the experimental and theoretical aspects of the phenomenon are examined to illustrate the current status of the field.

1. INTRODUCTION

During the past three decades the explosive progress in the area of electronic and photonic devices has been possible largely because of technological advances in the growth and physical understanding of semiconductor alloys. The silicon-germanium heterojunction bipolar transistor, high electron mobility transistor, light emitting diode, semiconductor diode laser and solar cell are illustrative examples of the pivotal role alloy semiconductors have played as precursors of whole new technologies. The relentless pursuit towards miniaturization of electronic devices and the recent excitement in nanoscience and nanotechnologies have generated a demand for a much better understanding of semiconductor alloys and their properties at ultra-short length scales. Although there have been

significant advances made in understanding the physical properties of alloys on a macroscopic scale, it is anticipated that on a submicroscopic scale certain peculiarities will be manifested. Although the conventional approach to treating semiconductor alloys as substitutional solid solutions has yielded satisfactory results for macroscopic physical properties, it is unclear how this will breakdown due to the more violent effects of statistical fluctuations at the nanoscale. With regard to theoretical modeling, there has been a need for experimental guidance but little progress made due to the paucity of techniques for exploring this realm. The phenomenon of spontaneous ordering appears well suited for exploring the physical consequences of disorder because it provides a convenient avenue for controlling statistical fluctuations. The ability to controllably achieve desired order parameters using this process allows for the possibility of tailored disorder in a lattice and there has been a great deal of excitement towards understanding how the consequences of this tunable disorder are manifested on the electronic and optical properties of spontaneously ordered alloys. For example, one can choose to tailor disorder on the cation or anion sublattice and study the consequences this has on the scattering of Bloch states, phonons, and excitons. Spontaneous ordering changes the alloys symmetry which in turn brings about changes to the electronic and optical properties. Bandgap lowering, valence band splitting, effective mass anisotropy, birefringence, electron spin polarization, second harmonic generation and spontaneously generated electric fields are examples of such intrinsic symmetry induced changes that have been investigated in the past. The intrinsic effects that are the results of the alternation in statistical fluctuations in partially ordered alloys have received much less attention. These include the effects of alloy scattering on mobility, exciton linewidth, and lattice dynamics. The process of spontaneous ordering is inevitably associated with the formation of structural defects comprised of anti-phase boundaries, orientational domain boundaries, and spatial variations in the order parameter. These inherent microstructural changes that are extrinsic to the phenomenon of spontaneous ordering have been associated with peculiarities in the low temperature photoluminescence spectra, the formation of orientational superlattices, and the cancellation of spontaneous electric fields that have been predicted to exist in ordered alloys. Finally, the effect of spontaneous ordering on the band alignment between GaInP and GaAs has become the subject of recent investigation because of the manner in which this effects the performance of GaInP/GaAs heterojunction bipolar transistors.

Spontaneous ordering is a result of a short wavelength instability that results in a special point at a Brillouin zone boundary along the ordering axis collapsing onto the Brillouin zone center. The process as observed in epitaxially grown semiconductor alloys is irreversible but results in group-

subgroup relations characteristic of the Landau theory of structural phase transformations. Here, as opposed to ordering in bulk grown crystals, ordering is initiated at the surface of the epitaxially growing layer and as such is essentially controlled by kinetics and thermodynamics at the growth surface. It is the two dimensional structural transformation at the surface that evolves into the final observed three dimensional structural transformation. In-situ optical characterization techniques such as Reflectance Difference Spectroscopy and Surface Photoabsorption Spectroscopy that probe changes occurring at the growth surface have been used to investigate details of the ordering mechanism. In this chapter we will provide a brief review of the various studies that have been done as regards the intrinsic and extrinsic changes to the electronic and optical properties that result from spontaneous ordering in epitaxially grown semiconductor alloys. The focus will primarily be on the alloy GaInP because this system has proven to be most amenable to experimental investigation

2. ORDERING INDUCED BAND GAP REDUCTION AND VALENCE BAND SPLITTING

2.1 Band Gap Reduction

Long before CuPt ordering was actually observed in III-V semiconductors[1-13], Pikhtin[14] had already noticed the scatter in the values for the band gap of GaInP in the literature, and pointed out that it was possible that the disagreement between the experimental results obtained by different research groups for the $\text{Ga}_x\text{In}_{1-x}\text{P}$ system were due to some ordering components in these solid solutions resulting from specific growth techniques. For ordered GaInP alloy, a band gap reduction was first inferred from the red shift of the photoluminescence (PL) peak[9], and later confirmed by an absorption measurement[15] by Gomyo et al. However, it was not clear whether the GaInP samples were fully or partially ordered. The fact that CuPt ordered samples were found to have different band gaps[16-18] and valence band splittings[19] logically led to the recognition of the partial ordering in GaInP alloys[19]. The experimentally measured band gap reduction (< 100 meV typically) was found to be significantly smaller than the band gap bowing obtained from the earliest band structure calculations for a fully CuPt ordered $\text{Ga}_{0.5}\text{In}_{0.5}\text{P}$: 455 meV of Wei and Zunger[20], and 330 meV of Kurimoto and Hamada[21]. The band gap bowing was defined as the band gap difference between the average value of the binaries and the value for the actual structure, where the band gaps were calculated using a

self-consistent general-potential linear augmented-plane-wave (LAPW) method within the local-density-functional approximation (LDA)[20,21]. A direct comparison of these theoretical results with the experimental data was not possible without knowing the bowing for the disordered structure. However, the random structure was too difficult to calculate using this technique. Kurimoto and Hamada[21] believed that their result was in good agreement with the experimental data of Ref.[9], by assuming a large bowing already existing for the random structure. Wei and Zunger[20] pointed out a large discrepancy between the experimental result of Ref.[9] and their calculation. A few hypothesis were given for the discrepancy[20]: (1) partial ordering, (2) coexistence of different types of ordering, and (3) antiphase boundaries. Later, the band gap of the random structure, simulated by a so-called quasi-random structure (SQS)[22], was calculated using the LAPW method[23,24]. The band gap reduction for the fully ordered structure was calculated by Wei et al to be $\delta E_g(x = 0.5, \eta = 1) = E_g(x = 0.5, \eta = 0) - E_g(x = 0.5, \eta = 1) = 320 \text{ meV}$ [24], where η is the order parameter that can vary from 0 to 1. Note that the accuracy of this value relies on three assumptions: (1) the quasi-random structure can adequately simulate the random structure, (2) the LDA error is negligible for the energy separations among different conduction band critical points, and (3) the LDA error is approximately the same for different structures (either the random or ordered). Since the samples are only partially ordered (i.e., $(\eta < 1)$), to compare experimental data with the above theoretical calculation one needs to (1) determine the order parameter experimentally and (2) know the functional form for $\delta E_g(x, \eta)$. Two approaches have been used to obtain the functional form of $\delta E_g(x, \eta)$: one is to directly calculate $\delta E_g(x, \eta)$ for different values of x and η [25-27], and the other is to seek an interpolation function between the end points $\eta = 0$ and 1[23]. Note that if one only knows the functional form but not the order parameter of the sample, the comparison is still impossible, although one may find such comparisons with claimed good agreements in the literature. Although the results of direct calculations by Capaz and Koiller[25] and by Mäder and Zunger[26] have been available for quite some time, the most widely used functional form for $\delta E_g(x, \eta)$ has been the so-called η^2 rule proposed by Laks et al[23]: $P(x, \eta) = P(x, 0) + \eta^2 [P(X_\sigma, 1) - P(X_\sigma, 0)]$, where X_σ is the composition of the ordered structure. The combination of this scaling rule and the end-point value of $\delta E_g(0.5, 1) = 320 \text{ meV}$ has been extensively used for determining the order parameter of partially ordered samples. An indirect but meaningful method of making the comparison between experiment and theory was suggested by Zhang and Mascarenhas[28]: assuming the validity of the η^2 rule, the ratio $r = \delta E_g(\eta)/\Delta_{CF}(\eta) = \delta E_g(\eta = 1)/\Delta_{CF}(\eta = 1)$ should be a constant, and can be compared with experimental data. Here $\Delta_{CF}(\eta = 1)$ is the crystal-field

splitting parameter for the fully order structure at $x = 0.5$. Utilizing the piezo-reflectance data of Alonso et al[29], they found $r = 2.0 \pm 0.1$ [28]. Subsequently, more accurate experimental data of Ernst et al[30] (measured by PL excitation, PLE, spectroscopy) yielded $r = 2.36 \pm 0.06$, and of Fluegel et al[31] (measured by differential absorption using a time-resolved pump-probe technique) yielded 2.66 ± 0.15 . Comparing to the theoretical value of $r = 1.6$ (with $\Delta_{CF}(1) = 0.20$ eV)[24], these experimental data indicated that the theory of Ref. [24] either underestimated $\delta E_g(1)$ or overestimated $\Delta_{CF}(1)$. A revised calculation of Wei and Zunger[32] has given new values of $\delta E_g(1) = 430$ meV and $\Delta_{CF}(1) = 160$ meV, resulting in $r = 2.69$, which is in good agreement with the experimental result.

Despite the good agreement that has been achieved in the above-mentioned comparison, it is still not possible to make a direct comparison of any individual physical property for a partially ordered sample. Another concern relates to how accurate the η^2 rule really is. Two techniques, NMR[33,34] and x-ray diffraction[35,36], have been used for determining the order parameter experimentally. For the NMR technique, two approaches have been adopted. One used by Tycko et al[33] was to analyze the relative areas of the ^{31}P NMR lines (there are five lines corresponding to five possible $\text{Ga}_n\text{In}_{1-n}\text{P}$ clusters with $n = 0 - 4$). They found $\eta \leq 0.6$ for the ordered samples studied, but no explicit η dependence was given. The other used by Mao et al[34] was to analyze the NMR spin echo of ^{71}Ga with the help of a point-charge model. Only the result of one sample was given with relatively large error bars. Wei and Zunger[37] later pointed out that the point-charge model used in Ref.[34] was inadequate for modeling the experiment. The x-ray technique is perhaps the most traditional technique that has been used for the measurement of order parameters. Forrest et al[35] successfully applied this technique, in conjunction with optical measurements, to obtain the dependence of the band gap reduction and valence band splitting as a function of order parameter. Using the η^2 rule, they were able to get by extrapolation the end-point values of $\delta E_g(1) = 498 \pm 27$ meV and $\Delta_{CF}(1) = 189 \pm 11$ meV. These values are in fact the first experimentally obtained band structure parameters for the currently unachievable fully ordered GaInP. However, one has to remember that the validity of these values relies on the validity of the η^2 rule. In addition to this concern, a very recent x-ray diffraction study of Li et al[36] indicates that the domain size affects the order parameter derived from the modeling method used in Ref.[35] for samples with small domain sizes. A systematic investigation of this issue has not yet been accomplished.

The results of two early direct calculations[25,26] of the band gap for partially ordered structures ($0 < \eta < 1$) had largely been ignored, because of the convenient use of the η^2 rule proposed by Laks et al[23]. The result of

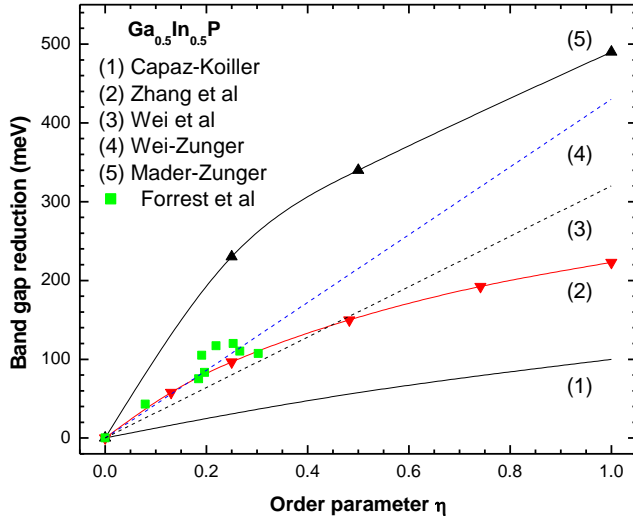


Figure 1. A comparison of the band gap reduction vs. order parameter between theoretical calculations and the experimental data. Theoretical results are from Ref.[25] (Capaz and Koiller), Ref.[27] (Zhang et al), Ref.[24] (Wei et al), Ref.[32] (Wei and Zunger), and Ref.[26] (Mäder and A. Zunger). Experimental data are from Ref.[35] (Forrest et al).

Ref.[25], $\delta E_g(\eta) = 130 \eta^2 - 30 \eta^4$ (meV), appears to have underestimated the band gap reduction, but this was the first attempt to directly calculate $\delta E_g(\eta)$. The result of Ref.[26], in fact, shows a strong deviation from the η^2 rule for $\delta E_g(\eta)$, but its end point value $\delta E_g(1) = 490$ meV appears to be in very good agreement with the extrapolated value of Forrest et al[35] using the η^2 rule, which presents an apparent paradox. The most recent calculation of Zhang et al[27] has yielded a value for $\delta E_g(\eta)$ that is in very good agreement with the experimental data of Forrest et al[35] available for $\eta < 0.55$, but severely deviates from the η^2 rule for $\eta > 0.5$, with an end point value $\delta E_g(1) = 223$ meV.

Fig.1 compares $\delta E_g(\eta)$ obtained from all the three direct calculations[25-27], the η^2 rule[24,32], and the experimental data[35]. Among the three direct calculations, the most recently calculation of Zhang et al[27] appears to best match the experimental data. In this empirical pseudopotential calculation, the partial ordering has been more realistically modeled by using a $\sim 3,500$ atoms size supercell and averaging over 100 configurations, compared to Capaz and Koiller's tight binding calculation[25] using a 64 atom size unit cell and averaging over 400 structures or Mäder and Zunger's

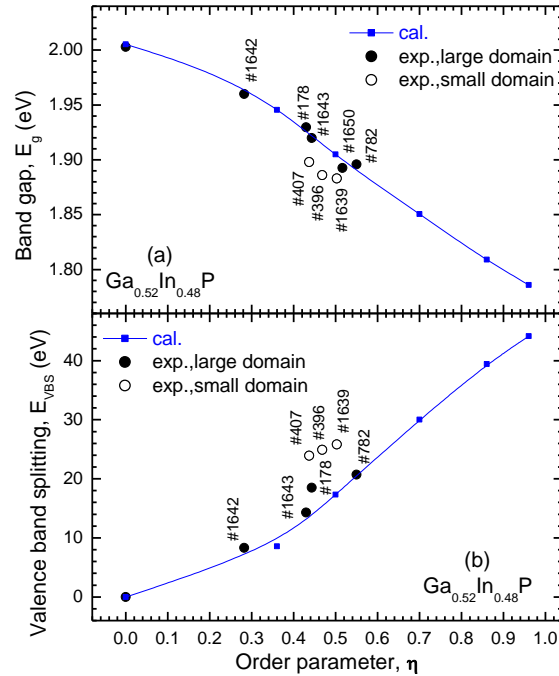


Figure 2. Band gap (E_g) and valence band splitting ($E_{v,as}$) as functions of order parameter η for partially ordered $\text{Ga}_{0.52}\text{In}_{0.48}\text{P}$ alloys. Theoretical curves are from Ref.[27] (Zhang et al). Experimental data are from Ref.[35] (Forrest et al), except for data points for #178 and #782 (J. H. Li et al, unpublished).

pseudopotential calculation[26] using 32 atom size quasi-random structures. The empirical pseudopotential method of Ref. [27] so far is the only method capable of calculating the absolute band gap energy as a function of order parameter in good agreement with experimental data.

Fig.2 shows a comparison for the absolute band gap energy between the experimental data and the theoretical results for $x_{\text{Ga}} = 0.52$ (at which $\text{Ga}_x\text{In}_{1-x}\text{P}$ is lattice matched to GaAs). One can see in Fig.2 that the data for samples with small crystalline domains do not agree with the theoretical curve as well as the data for samples with large domains. It is worth mentioning that the direct calculation of Ref.[27] confirms that the crystal field splitting parameter, $\Delta_{\text{CF}}(\eta)$ does obey the η^2 rule. Although without experimental data for higher ordered samples, it is hard to judge which results of Ref. [27] and Ref.[32] for the band gap reduction is more accurate for $\eta > 0.55$, there is a logical difficulty in believing that the η^2 rule should be valid for the large η region[27]. If one views ordering as a perturbation of the random alloy, this perturbation causes a folding of the Brillouin-zone L point to the Γ point,

and the repulsion between the folded L state and the original conduction band edge state may be considered as the primary contribution to the band gap reduction. A perturbation scheme proposed by Wei and Zunger[20] gives $\delta E_c \propto |\langle c, L | \Delta V | c, \Gamma \rangle|^2 / (E_{cL} - E_{c\Gamma})$. If the matrix element $|M_{L\Gamma}| = |\langle c, L | \Delta V | c, \Gamma \rangle| \propto \eta$, one does have $\delta E_c \propto \eta^2$. However, to achieve the large band gap reduction of ~ 400 meV[32], the coupling would be too strong for this perturbation scheme to be valid, considering the fact that $\delta E_{L\Gamma} = E_{cL} - E_{c\Gamma}$ is ~ 350 meV for the random alloy. Thus, a higher order theory would naturally be expected to bring in higher order terms beyond the η^2 term. In general, without actually performing the calculation, it is not trivial to make a judgment as to whether or not a physical quantity $\Pi(x, h)$ should follow the η^2 rule. An obvious reason for not taking the validity of η^2 rule for granted is that physical properties are not always linearly related to each other. Thus, their relationship to η^2 is not guaranteed to be linear, unless the ordering effect is very weak. In fact, as will be discussed in the next subsection, the dependence of the valence band splitting on η is a good example of how a more complicated η dependence emerges from the strong interaction amongst the valence bands, even though the crystal field splitting parameter $\Delta_{CF}(\eta)$ involved does obey the η^2 rule.

2.2 Valence Band Splitting

The ordering induced valence band splitting was first observed in a polarized PL measurement at room temperature by Mascarenhas et al[19]. Kanata et al obtained the valence band splittings for a set of samples with varying degree of order through temperature dependent PL measurements[38]. Usually, because of the involvement of the Boltzmann occupation factor in the emission process, PL is a less accurate technique for determining the critical points, comparing to other techniques like PLE spectroscopy[30,38,39] and modulation spectroscopy (electroreflectance[40], piezoreflectance[29], and differential absorption[31]). PLE could resolve the split valence band quite accurately, but could not access the spin orbit band. All the modulation techniques could resolve all the three valence band states near the band edge, but electroreflectance as well as piezoreflectance generally require a complex fitting procedure. The time-resolved pump-probe differential absorption technique used by Fluegel et al[31] appears to be the most accurate technique for this purpose. Fig.3 shows the experimental data obtained by PL[38], piezoreflectance[29], PLE[30], and differential absorption[31]. Fluegel et al[31] also found the spin-orbit splitting parameter $\Delta_{SO} = 103$ meV to be independent of the order parameter (up to $\eta \sim 0.6$).

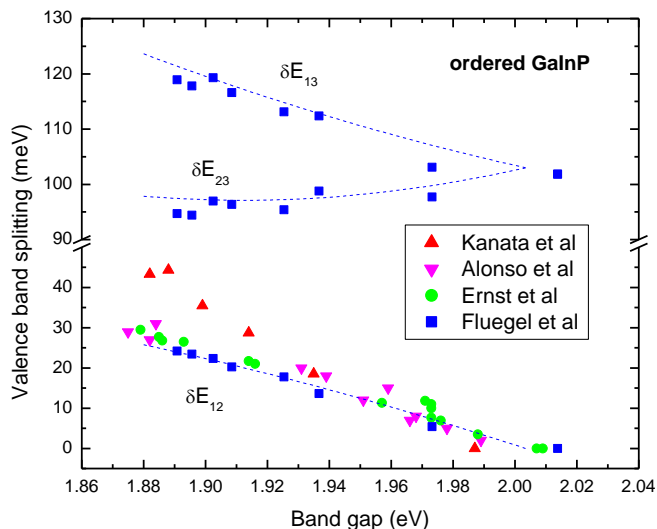


Figure 3. A comparison of the valence band splitting vs. the band gap reduction determined by using different experimental techniques: photoluminescence (Ref.[38] of Kanata et al), piezoreflectance (Ref.[29] of Alonso et al), photoluminescence excitation (Ref.[30] of Ernst et al), and differential absorption (Ref.[31] of Fluegel et al).

The valence band splitting can be approximately but conveniently described by the quasicubic model which was originally proposed by Hopfield for treating simultaneous perturbations of a uniaxial crystalline field and spin-orbit coupling to the triply degenerate Γ_{15} valence band[41]. This model had been used by Shay et al[42] for describing the valence band splitting and optical polarization in chalcoprite ordered ZnSiAs_2 crystals. Not only had they pointed out that the valence band splitting and polarization dependence agreed with observations in stressed zinc-blende crystals, but also they used the concept of zone folding by stating “much additional structure is observed in ZnSiAs due to pseudodirect band gaps which result from the doubling of unit cell in chalcopyrite relative to zinc-blende. This change in the unit cell causes the Brillouin zone of zinc-blende to be imbedded into the smaller Brillouin zone of chalcopyrite”. Wei and Zunger[43] and others[28,44] applied this model to CuPt ordered III-V alloys. The three valence band edge states are given as follows:[41-44]

$$E_1 = \frac{\Delta_{CF}}{3}, \quad (1)$$

$$E_{2,3} = -\frac{1}{2}(\Delta_{SO} + \frac{\Delta_{CF}}{3}) \pm \frac{1}{2}[(\Delta_{SO} + \Delta_{CF})^2 - \frac{8}{3}\Delta_{SO}\Delta_{CF}]^{1/2}, \quad (2)$$

where the energy reference is the valence band maximum with spin-orbit interaction taken into account. Based on the calculations of Ref.[43] or Ref.[24], it was unclear whether the ordering caused any shift in the center of gravity of the valence band. The recent empirical pseudopotential calculation of Zhang et al[27] has yielded $\Delta_{CF}(1) = 135$ meV and a net valence band upward shift of 30 meV for $\eta = 1$. Thus, the center of gravity actually moves downward by 15 meV. Although for most optical measurements the relevant parameter is the band gap change, the absolute shift of the band edge, which determines the band offset, is important for understanding phenomena involving heterostructures (e.g., ordered GaInP/GaAs). Issues related to the ordering induced change in band offsets will be discussed later. Note that in Eq.(1) and (2) the spin-orbit splitting is assumed unchanged with ordering. In general, the spin-orbit interaction may change due to ordering. Then, Eq.(1) and (2) should be modified accordingly[28], in analogy to the situation for the effect of strain.

3. ORDERING INDUCED OPTICAL ANISOTROPY OR POLARIZATION

3.1 Linear Polarization

Since ordering reduces the crystal symmetry from T_d for the random alloy to C_{3V} for the CuPt structure, selection rules for various types of optical transitions are expected to change. The symmetry effect was first demonstrated in a polarized PL measurement[19], and later in various polarized spectroscopic studies which include PLE[19,30,39,45], cleaved edge PL[46,47], piezo-reflectance[29], reflectance difference[48], electroreflectance[40], electroabsorption[49], photocurrent[50], ellipsometric measurement[51], second harmonic generation[52], and birefringence[53-55]. The ordering induced optical anisotropy has also been used advantageously for making various polarization selective or sensitive devices such as polarization rotators[53,55], lasers[56], LEDs[57], and optical switches[58]. As mentioned above, the ordering induced perturbation to the random alloy is closely analogous to that of uniaxial strain to a zinc-blende semiconductor. Thus, the well developed perturbation theory[59] for

strain can be readily used for calculating the ordering induced valence band splitting and the interband optical transition probability[28,56,60-62]. The three most frequently encountered optical transitions are those from the three valence bands to the conduction band. If there is no epitaxial strain in the ordered layer (i.e., the epilayer is lattice matched to the substrate), the transition intensity, which is proportional to the square of the interband transition matrix element, are given in the following analytical forms[61]:

$$I_1 = e_1^2 + e_2^2 \quad (3)$$

for the transition between the topmost valence band (the heavy hole like) and the conduction band,

$$I_2 = \frac{2a_2^2}{3} + \frac{(a_1^2 + 2\sqrt{2}a_1a_2)}{3}(e_1^2 + e_2^2) + \frac{4(a_1^2 - \sqrt{2}a_1a_2)}{3}e_3^2 \quad (4)$$

for the transition between the second valence band (the light hole like) and the conduction band, and

$$I_3 = \frac{2b_2^2}{3} + \frac{(b_1^2 + 2\sqrt{2}b_1b_2)}{3}(e_1^2 + e_2^2) + \frac{4(b_1^2 - \sqrt{2}b_1b_2)}{3}e_3^2 \quad (5)$$

for the transition between the third valence band (the spin-orbit split-off band) and the conduction band, where $\mathbf{e} = (e_1, e_2, e_3)$ is a unit vector in the direction of the light polarization in a coordinate system (x' , y' , z') with z' along the ordering direction [111], x' and y' in the plane perpendicular to the ordering direction ($x' \sim [11\bar{2}]$ and $y' \sim [\bar{1}10]$). The four coefficients in the above equations are $a_1 = (E_3 + d) / \sqrt{(E_3 + d)^2 + 2d^2}$, $a_2 = -\sqrt{2}d / \sqrt{(E_3 + d)^2 + 2d^2}$, $b_1 = (E_2 + d) / \sqrt{(E_2 + d)^2 + 2d^2}$, $b_2 = -\sqrt{2}d / \sqrt{(E_2 + d)^2 + 2d^2}$, where $d = -\Delta_{CF}/3$. Fig.4 shows how the transition intensity varies with the strength of ordering, measured by the crystal field splitting parameter, for the two frequently encountered polarizations in the growth plane[61].

There had been a few attempts[40,60] to make quantitative analyses of the experimental data by using the theoretical results like that of Fig.4. However, it was later shown[61] that various other effects could result in significant deviations from the theoretical curves of Fig.4. For instance, the substrate tilt angle is a critical factor for quantitatively evaluating the optical anisotropy in two important aspects. Firstly, the crystalline structure strongly depends on the tilt angle. On an exact (001) substrate, two equally probable ordered variants tend to form quasi-periodic micro-domain twins[63,64]. Such a more complex form of ordering, termed an orientational superlattice by Mascarenhas et al[65,66], in fact has distinctly different electronic and optical properties from the simple single-variant

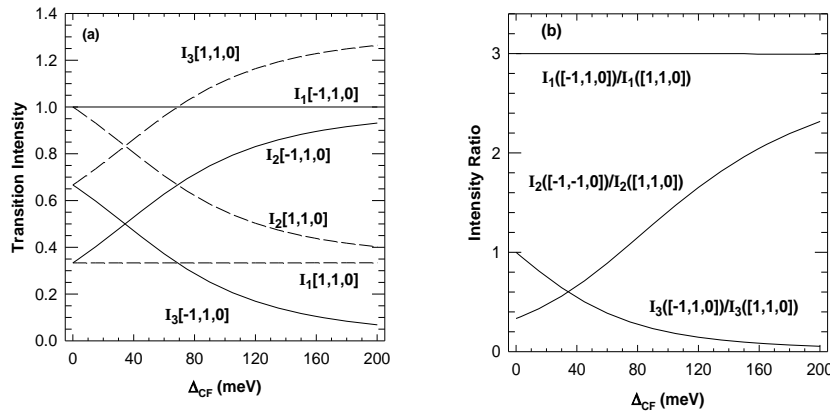


Figure 4. Calculated band-to-band transition intensities at $k = 0$ from the three valence bands to the conduction, respectively, with light polarized along the $[-110]$ and $[110]$ direction: (a) for the intensities and (b) for the intensity ratios. Curves are re-plotted from Fig. 4 of Ref.[61] (Zhang et al).

CuPt structure. It is, thus, quite inappropriate to apply the theory which is only meant for the CuPt structure to this special category of superlattices[67,68]. Secondly, the single-variant CuPt ordered structure can be obtained by using substrates tilted toward one of the $[111]_B$ directions, but the substrate tilt introduces a substantial effect on the polarization anisotropy[61]. For instance, the anisotropy ratio for the interband transition involving the topmost valence band is calculated to be $R_1 = 3$ between the two orthogonal $[110]$ directions[60], as shown in Fig.4(b). However, this ratio is expected to reduce to 2.3 for a sample grown on a $6^\circ B$ tilt substrate, when measured on the growth surface[61]. Also, the transition intensity shown in Fig.4 is calculated only for the electron-hole direct transition at $k = 0$. In reality, the excitonic effect is involved in the band edge transition, which requires knowledge of the transition matrix element at $k \neq 0$ [61]. Fig.5 shows typical polarized PL spectra for a pair of (nearly) random and ordered GaInP samples. The polarization ratio for the band edge excitonic transition is found to be ~ 2.0 , instead of 3, for the ordered sample, almost independent of the order parameter for samples with reasonably large order parameters[61]. Such a result indicates that to quantitatively analyze the optical anisotropy one has to take into account the factors of substrate tilt (both orientation and angle), excitonic effect, and even epitaxial strain. It is worth pointing out that in all the above-mentioned theoretical considerations for the interband transition intensity, the conduction band wavefunction has been assumed unchanged with the occurrence of ordering. Since CuPt

ordering causes a mixing of the Γ and folded L point, it is expected that transition intensity should decrease on increasing the degree of order. Such an effect can be estimated by using the coupling matrix element given in Ref.[27].

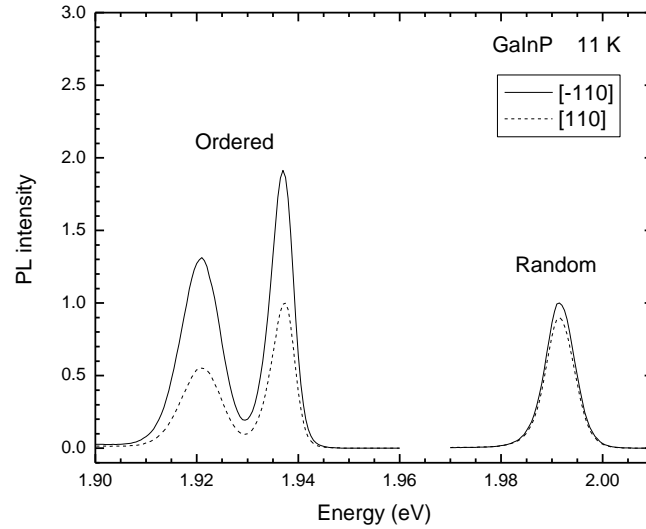


Figure 5. Typical polarized photoluminescence spectra for a random and a partially ordered GaInP alloy. Spectra are re-plotted from Fig.1 of Ref.[61] (Zhang et al).

3.2 Circular (Spin) Polarization

It is well known that for a zinc-blende semiconductor near-band-edge interband optical pumping by circularly polarized light can produce conduction band electrons with a maximum degree of polarization $P = (n_{\uparrow} - n_{\downarrow}) / (n_{\uparrow} + n_{\downarrow}) = 50\%$, owing to the opposite polarization for electrons transferred from the degenerate heavy and light hole state[69]. It was pointed out by Ciccacci et al[70] that for a CuAu ordered AlGaAs alloy (i.e., GaAs/AlAs monolayer superlattice) 100% polarization could be achieved for the electrons, because of the ordering induced valence band splitting. Wei and Zunger[60] extended this idea to the CuPt ordered alloy. Experimentally, Kita et al[71] studied spin polarization of the band edge excitonic luminescence pumped along the [001] direction. The maximum polarization, measured at nearly zero time delay, was found to be $\sim 55\%$. The primary reason given for the maximum polarization being significantly less than 100% was that the direction of the optical pumping was not along the ordering direction. Indeed, the maximum electron polarization for [001]

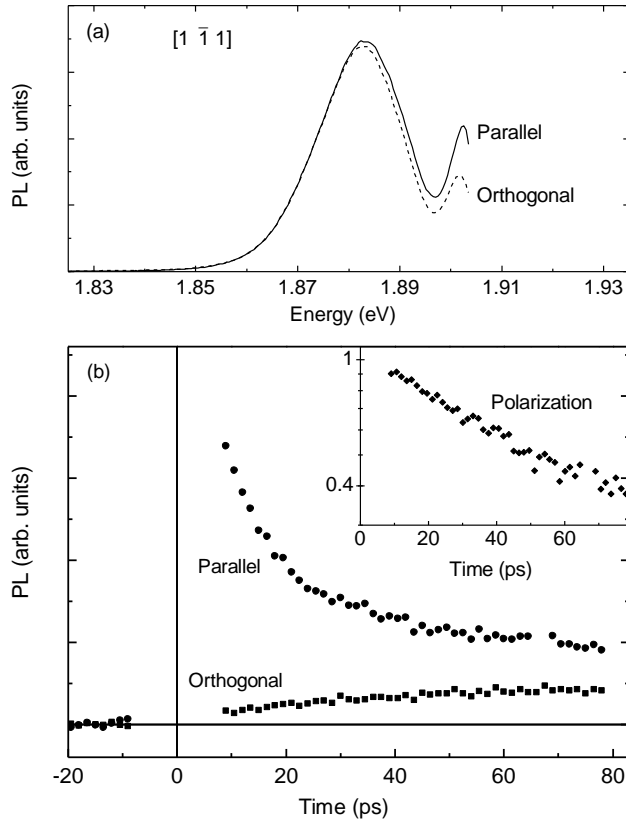


Figure 6. Spin polarization pumped and measured along the ordering direction. (a) Time-integrated photoluminescence (PL) spectra polarized parallel and orthogonal to the circularly polarized pump; and (b) time-resolved PL at the peak of the band edge excitonic transition, under identical conditions. Inset: log plot of degree of polarization (from Ref.[72] of Fluegel et al).

optical pumping P_{001} is only 50%, which can be evaluated using the following wavefunctions for the doublet degenerate topmost valence band state:

$$\varphi_1 = \frac{1}{\sqrt{2}} \left| \frac{3}{2}, -\frac{3}{2} \right\rangle_{(001)} + \frac{1-i}{\sqrt{6}} \left| \frac{3}{2}, -\frac{1}{2} \right\rangle_{(001)} + \frac{i}{\sqrt{6}} \left| \frac{3}{2}, \frac{1}{2} \right\rangle_{(001)}, \quad (6)$$

$$\varphi_2 = \frac{i}{\sqrt{6}} \left| \frac{3}{2}, -\frac{1}{2} \right\rangle_{(001)} + \frac{1+i}{\sqrt{6}} \left| \frac{3}{2}, \frac{1}{2} \right\rangle_{(001)} + \frac{1}{\sqrt{2}} \left| \frac{3}{2}, \frac{3}{2} \right\rangle_{(001)}. \quad (7)$$

One should note that the PL polarization, which differs from the polarization of the electron populations, not only depends on the polarization of the electrons but also on that of the holes. If the spin orientation of holes is assumed unrelaxed for near band edge pumping, the maximum value for the PL polarization with an exact [001] pumping is expected to be 75% [69]. In fact, Fluegel et al [72] showed that even for pumping along the direction normal to the sample surface, at zero time delay, the PL polarization could approach values as high as 90%, which can be explained by taking into account the 6° substrate tilt angle as well as a finite collection angle of similar amount. Furthermore, Fluegel et al [72] actually performed the spin-polarized PL measurement pumped exactly along the ordering direction. In this case, as shown in Fig.6, a near 100% polarization at zero time delay was in fact observed.

4. ORDERING INDUCED CHANGES IN EFFECTIVE MASS

The first attempt by Jones et al [73] to study the effect of ordering on the effective mass using magneto-photoluminescence indicated that the exciton reduced mass of an ordered sample was smaller than that of a disordered sample. The change of the reduced mass was attributed to the reduction of the conduction band effective mass. Emanuelsson et al [74] subsequently measured the electron effective mass of an ordered and a disordered sample by optically detected cyclotron resonance measurements, and found $m_c = 0.088 \pm 0.003$ for the ordered sample and $m_c = 0.092 \pm 0.003$ for the disordered sample. In both of these studies, the reduction of the conduction band mass was explained as being a result of ordering induced band gap reduction using a $\mathbf{k}\cdot\mathbf{p}$ model. It was later pointed out by Raikh and Tsiper [75] for the conduction band and Zhang and Mascarenhas [28] for the valence band that ordering not only modifies the effective mass but also makes it anisotropic. Thus, any magneto-measurement should be sensitive to the direction of the field. The conduction band effective mass m_c was derived by Raikh and Tsiper as follows, with only the repulsion between the conduction band and the folded L-band considered [75]:

$$\frac{1}{m_{c\parallel,\perp}} = \frac{1}{2m_\Gamma} \left(1 + \frac{\delta E_{\Gamma L}}{\sqrt{\delta E_{\Gamma L}^2 + 4M_{\Gamma L}^2}} \right) + \frac{1}{2m_{L\parallel,\perp}} \left(1 - \frac{\delta E_{\Gamma L}}{\sqrt{\delta E_{\Gamma L}^2 + 4M_{\Gamma L}^2}} \right), \quad (8)$$

where m_Γ (m_L) is the conduction band effective mass at Γ (L) point for the disordered alloy, and m_\parallel and m_\perp represent the effective mass parallel and perpendicular to the ordering direction, respectively. Assuming $m_{L\parallel} > m_{L\perp} >$

m_Γ , the authors found $m_{c\parallel} > m_{c\perp} > m_\Gamma$, i.e., the conduction band effective mass of an ordered structure would always be heavier than that of a disordered structure, and it is more heavier along the ordering direction. However, Zhang and Mascarenhas pointed out[28] that the coupling to the valence would reduce m_c and, in the process, cause m_c to be anisotropic. The following results were derived[28]:

$$\frac{1}{m_{c\parallel}} = \frac{1}{m_\Gamma} + \frac{E_p}{3} \left(\frac{2a_0}{E_g^2} + \frac{a_0}{E_d^2} \right) - \frac{2E_p}{9} \left(\frac{\Delta_{CF}}{E_g^2} + \frac{2\Delta_{CF}}{E_g E_d} \right), \quad (9)$$

$$\frac{1}{m_{c\perp}} = \frac{1}{m_\Gamma} + \frac{E_p}{3} \left(\frac{2a_0}{E_g^2} + \frac{a_0}{E_d^2} \right) + \frac{E_p}{9} \left(\frac{\Delta_{CF}}{E_g^2} + \frac{2\Delta_{CF}}{E_g E_d} \right), \quad (10)$$

where $a_0 = \delta E_v - \delta E_c = \delta E_g - \Delta_{CF}/3$ (here $\delta E_g > 0$) is the band gap reduction caused by the shift of the conduction band and the shift of the center of gravity of the valence band, and $E_d = E_g + \Delta_{SO}$. In principle, one could combine the two effects described by Eq.(8) – (10), but a few key parameters (e.g., m_L , $\delta E_{\Gamma L}$ and $M_{\Gamma L}$) are not so well known. Nevertheless, both effects considered above would make $m_{c\parallel} > m_{c\perp}$. Later, Franceschetti et al[76] used a first-principles method to calculate the effective mass for the fully ordered structure. They found that $m_{c\parallel}$ increased significantly while $m_{c\perp}$ slightly decreased from m_Γ . However, ambiguities arose when the authors attempted to generate interpolation curves between $\eta = 0$ and 1, because the validity of the η^2 rule was uncertain. It now appears unlikely to be true[27]. Even if the η^2 rule was valid, there was an ambiguity as to whether the rule should have been applied to m_c itself or to the energy $E_c(k) \propto 1/m_c$.

The valence band effective masses were derived analytically in Ref.[28]. For the topmost (heavy-hole like) valence band,

$$\frac{1}{m_{hh\perp}} = \gamma_1 + \gamma_3 + \frac{\delta E_g E_p}{2E_g^2}, \quad (11)$$

$$\frac{m_e}{m_{hh\parallel}} = \gamma_1 - 2\gamma_3; \quad (12)$$

for the second (light-hole like) valence band,

$$\frac{1}{m_{lh\perp}} = \alpha_1(\gamma_1 - \gamma_3) - \alpha_2\gamma_1' + \alpha_3\gamma_3', \quad (13)$$

$$\frac{1}{m_{th\parallel}} = \alpha_1(\gamma_1 + 2\gamma_3) - \alpha_2\gamma_1' - 2\alpha_3\gamma_3'; \quad (14)$$

and for the spin-orbital split-off band,

$$\frac{1}{m_{sh\perp}} = \beta_1\gamma_1' - \beta_2\gamma_3' + \beta_3(\gamma_1 - \gamma_3), \quad (15)$$

$$\frac{1}{m_{sh\parallel}} = \beta_1\gamma_1' + 2\beta_2\gamma_3' + \beta_3(\gamma_1 + 2\gamma_3); \quad (16)$$

where

$$\alpha_1 = \frac{(2dx + 2\Delta_{so}d + 6d^2)}{x^2 - (\Delta_{so} - 3d)x}$$

$$\alpha_2 = \frac{(\Delta_{so} - d)x - \Delta_{so}^2 - 3d^2}{x^2 - (\Delta_{so} - 3d)x}$$

$$\alpha_3 = \frac{4\Delta_{so}d - 4dx - 12d^2}{x^2 - (\Delta_{so} - 3d)x}$$

$$\beta_1 = \frac{\Delta_{so}^2 + 3d^2 + (\Delta_{so} - d)x}{x^2 + (\Delta_{so} - 3d)x}$$

$$\beta_2 = \frac{-4\Delta_{so}d + 12d^2 - 4dx}{x^2 + (\Delta_{so} - 3d)x}$$

$$\beta_3 = \frac{2\Delta_{so}d + 6d^2 - 2dx}{x^2 + (\Delta_{so} - 3d)x},$$

and $x = [(\Delta_{so} + d)^2 + 8d^2]^{1/2}$. γ_1 , γ_3 , γ_1' , and γ_3' are Luttinger parameters. Qualitatively, one can conclude that (1) The “heavy-hole” mass m_{hh} along the ordering direction is indeed heavy, and independent of the degree of order; but in the ordering plane, m_{hh} is actually light and has a weak dependence on the order parameter. (2) Both the “light hole” mass m_{lh} and split-off band mass m_{sh} strongly depend on the order parameter, and show strong anisotropy. These valence band effective masses have later also been

calculated by Yeo et al with the spin-orbit coupling ignored[77], and by Tsitsishvili with the coupling to the conduction band ignored[62].

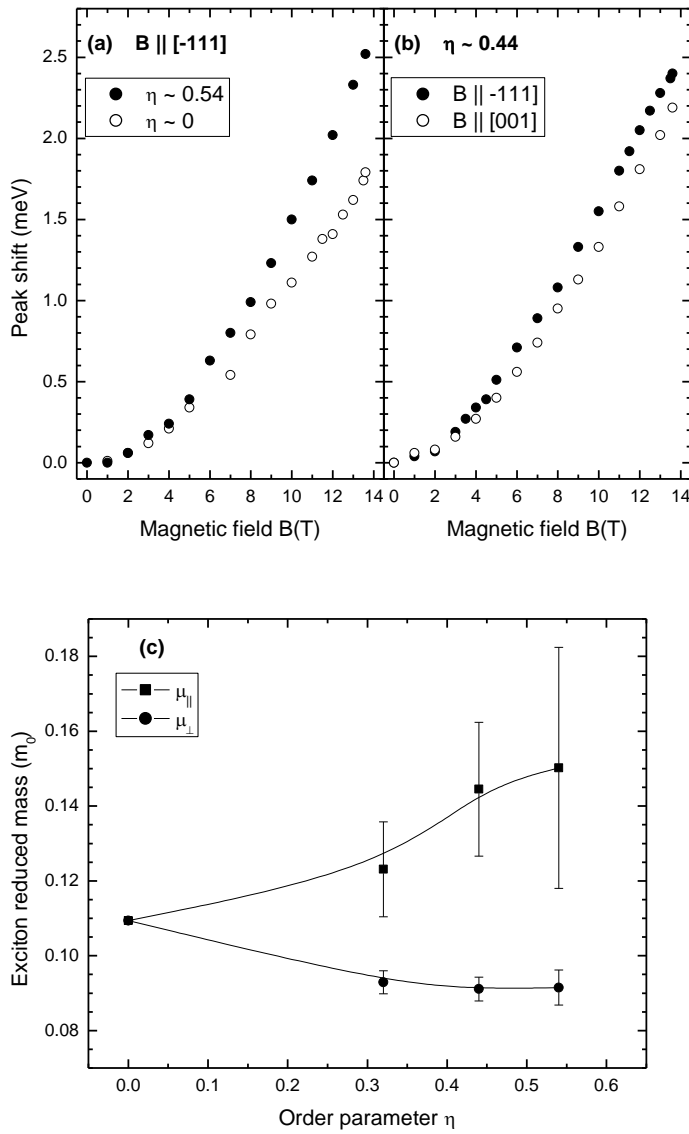


Figure 7. Results of a magneto-PL study on partially ordered GaInP alloys. (a) The effect of ordering indicated by the difference between the disordered and ordered sample in their energy shifts. (b) The effect of the effective mass anisotropy indicated by the difference in energy shift between two field directions. (c) Exciton reduced mass vs. order parameter, derived from the magnetic field induced peak shift (from Ref.[78] of Ernst et al).

The effective mass anisotropy was demonstrated by Ernst et al[78] using magneto-luminescence with the magnetic field oriented along either the $[\bar{1}11]$ ordering direction or the $[001]$ growth direction. As shown in Fig.7, they found that the diamagnetic shift (the shift of the excitonic emission energy) is larger with the field along the $[\bar{1}11]$ direction than when along the $[001]$ direction, as well as that the diamagnetic shift is larger for an ordered as compared to a disordered sample. The diamagnetic shift in the low field region can be described by the following perturbation formulae:

$$\delta E_{[\bar{1}11]} = \frac{e^2 B^2}{8\mu_{\perp} c^2} \langle f | x^2 + y^2 | f \rangle, \quad (17)$$

$$\delta E_{[001]} = \frac{e^2 B^2}{8\mu_{\perp} c^2} \frac{1}{3} \langle f | x^2 + y^2 + 2z^2 | f \rangle + \frac{e^2 B^2}{8\mu_{\parallel} c^2} \frac{1}{3} \langle f | x^2 + y^2 | f \rangle, \quad (18)$$

where μ_{\parallel} and μ_{\perp} are exciton reduced masses parallel and perpendicular to the ordering direction, and $f(x,y,z)$ is the exciton wavefunction at zero field. Applying these equations to the experimental data, exciton reduced masses were extracted, as shown in Fig.7(c). Zhang et al[79] later demonstrated that both μ_{\parallel} and μ_{\perp} could in fact be obtained from the experimental data with the field along the ordering direction alone, if the data for the entire range of field were modeled using a generalized theory. Given the fact that the effective masses of the topmost valence band are independent of or weakly dependent on the order parameter[28], the results for the reduced masses shown in Fig.7(c) should represent the trend of the variation of the conduction band masses. Thus, the variation of the conduction band masses appear to agree qualitatively, but not quantitatively, with the theoretical results of Ref.[76].

5. REFLECTANCE DIFFERENCE SPECTROSCOPY STUDY OF ORDERED STRUCTURE

Reflectance difference spectroscopy (RDS) has been used to investigate the anisotropic surface reconstruction of III-V materials with isotropic bulk properties[80]. This technique has been shown to also be a sensitive technique for detecting the presence of ordering in III-V alloys and can easily be adapted to *in situ* measurements during and after growth[48,81,82]. For the CuPt order structure, typically one measures the reflectance difference between the $[\bar{1}10]$ and $[110]$ direction (the ordering direction is assumed to be $[\bar{1}11]$), that is

$$\frac{\Delta R}{R} = \frac{R_{\bar{1}10} - R_{110}}{(R_{\bar{1}10} + R_{110})/2}, \quad (19)$$

where $R_{\bar{1}10}$ and R_{110} are the reflectances of light polarized along $[\bar{1}10]$ and $[110]$, respectively. The RD signal originates from the ordering induced anisotropy in the dielectric function ε which exhibits a uniaxial symmetry:

$$\varepsilon = \begin{pmatrix} \varepsilon_{\perp} & 0 & 0 \\ 0 & \varepsilon_{\perp} & 0 \\ 0 & 0 & \varepsilon_{\parallel} \end{pmatrix}, \quad (20)$$

where ε_{\parallel} and ε_{\perp} are dielectric functions for light polarized parallel and perpendicular to the ordering direction. For light incident normal to the (001) plane, the reflectances for the two orthogonal directions are[55]

$$R_{110} = \frac{|\sqrt{\varepsilon_{\perp}} - 1|^2}{|\sqrt{\varepsilon_{\perp}} + 1|^2}, \quad (21)$$

$$R_{\bar{1}10} = \frac{\left| \frac{\sqrt{\frac{\varepsilon_{\perp}\varepsilon_{\parallel}}{\bar{\varepsilon}}} - 1}{\sqrt{\frac{\varepsilon_{\perp}\varepsilon_{\parallel}}{\bar{\varepsilon}}}} \right|^2}{\left| \frac{\sqrt{\frac{\varepsilon_{\perp}\varepsilon_{\parallel}}{\bar{\varepsilon}}} + 1}{\sqrt{\frac{\varepsilon_{\perp}\varepsilon_{\parallel}}{\bar{\varepsilon}}}} \right|^2}, \quad (22)$$

where $\bar{\varepsilon} = (2\varepsilon_{\perp} + \varepsilon_{\parallel})/3$. Assuming $\delta\varepsilon = (\varepsilon_{\perp} - \varepsilon_{\parallel})/3 \ll \bar{\varepsilon}$, one approximately has $\Delta R/R \propto -2\delta\varepsilon \approx \varepsilon_{\bar{1}10} - \varepsilon_{110}$. Another commonly adopted approximation is to neglect the contribution of the imaginary part of the dielectric function near the fundamental band gap. The real part ε_1 takes the general form of[83]

$$\varepsilon_1 \propto E^{-2} [2\sqrt{E} - \sqrt{E_0 + E} - \sqrt{E_0 - E}\theta(E_0 - E)]. \quad (23)$$

There have been three iteratively improved models for modeling the near band-edge RD spectrum of a CuPt ordered GaInP alloy. Luo et al[48,81] first used a four-band model, Wei and Zunger[84] then used a six-band model. In all these approaches, the first two terms in Eq.23 were not included. It was later found out by Luo et al[85] that these two terms are critical for getting the sign correct for the calculated lineshape function above the band gap. It was also showed[85] that it was necessary to take into account the k-dependence of the interband transition matrix element in

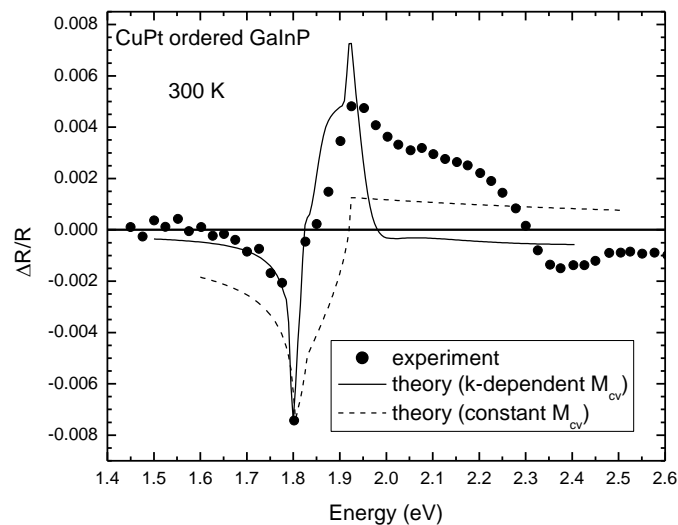


Figure 8. A comparison of an experimental reflectance difference spectrum and calculated lineshape functions with a constant or k -dependent interband transition matrix element. Curves are re-plotted from Fig.2 of Ref.[85] (Luo et al).

order to achieve an overall good agreement between the experimental data and the theoretical lineshape function. Fig.8 shows the comparison between an experimental RD spectrum and the calculated lineshape functions.

Since RDS is sensitive to the bulk anisotropy due to the ordering as well as the surface anisotropy that may exist in a zinc-blende structure, Luo et al[85] has managed to suppress the surface induced features in order to reveal the effect of bulk ordering near the band gap. However, the surface effect may contain information related to the formation mechanism of ordering. Zorn et al[86] have in turn applied RDS to investigate the correlation between CuPt ordering and surface reconstruction. They concluded that there was a clear and unambiguous correlation between the occurrence of ordering and the presence of P-dimers with a (2×1) surface reconstruction during growth, which would agree with the theoretical model of Zhang et al[87]. It is worth pointing out that the validity of this conclusion critically depends on the reliability of the procedure and assumption for separating the bulk (band structure) effect and the surface effect. The major assumption was that the anisotropic contribution from the oxidized GaInP surface was only small and independent from the bulk ordering, which allowed them to obtain the contribution of the bulk ordering by subtracting the spectrum of a disordered sample from that of the ordered sample for the temperature range $T < 775$ K. The oxide layer was assumed to desorb at $T > 800$ K. Thus, the RD signal at $T > 800$ K only had the

ordering contribution due to either the surface or bulk effect. After the bulk contribution, obtained by extrapolating the lower temperature data, was subtracted, they were in principle left with the surface contribution of ordering. The focus was on a spectroscopy feature near 3 eV that was assumed to be associated with the (2x1) reconstruction, because the (2x1) reconstruction was simultaneously observed by a RHEED measurement for CBE (chemical beam epitaxy) grown samples. No independent theoretical justification was given for whether or not the (2x1) reconstruction would give rise to the ~ 3 eV peak. Furthermore, even though MOVPE samples did have the similar feature at ~ 3 eV, there was no guarantee that the same reconstruction existed in the MOVPE growth; since the ordering was observed only for the MOVPE but not for the CBE grown samples, logically there was no guarantee that the ordering was correlated to the (2x1) reconstruction, even if the reconstruction did exist for both growths. Thus, the conclusion of Zorn et al needs further verification.

Another technique – surface photoabsorption (SPA), has been used by Murata et al[88,89] for studying the ordering induced surface effect. In fact, this technique is very similar to RDS, when the difference of two polarizations is evaluated. Murata et al have suggested that (2x4) reconstruction was necessary for ordering. According to the theoretical model of Zhang et al[87], the (2x4) reconstruction can indeed generate CuPt ordering, but its efficiency is expected to be weaker than that of the (2x1) reconstruction. We would like to note that the possible bulk effect was not taken into account in Murata et al's analysis.

6. MICROSTRUCTURE OF ORDERED ALLOYS

Using atomic scale, cross-sectional scanning tunneling microscopy (STM) it is possible to directly observe atomic arrangements in III-V semiconductors. The technique has also been used to examine CuPt ordering in GaInP and GaInAs, and provided detailed information on the evolution, anisotropy and magnitude of the local order parameter and on atomically abrupt antiphase boundaries between different ordered domains. Cross-sectional STM has previously been used to study compositional fluctuations[90,91], isovalent intermixing[92-95], interfacial roughness[96-99] in a variety of III-V semiconductors. STM has also been used to investigate ordered GaInP[100,101] and to image the natural $(\text{InP})_1(\text{GaP})_1$ superlattice associated with CuPt_B ordering on an atomic scale. These previous studies have also found evidence of a new ordering arrangement

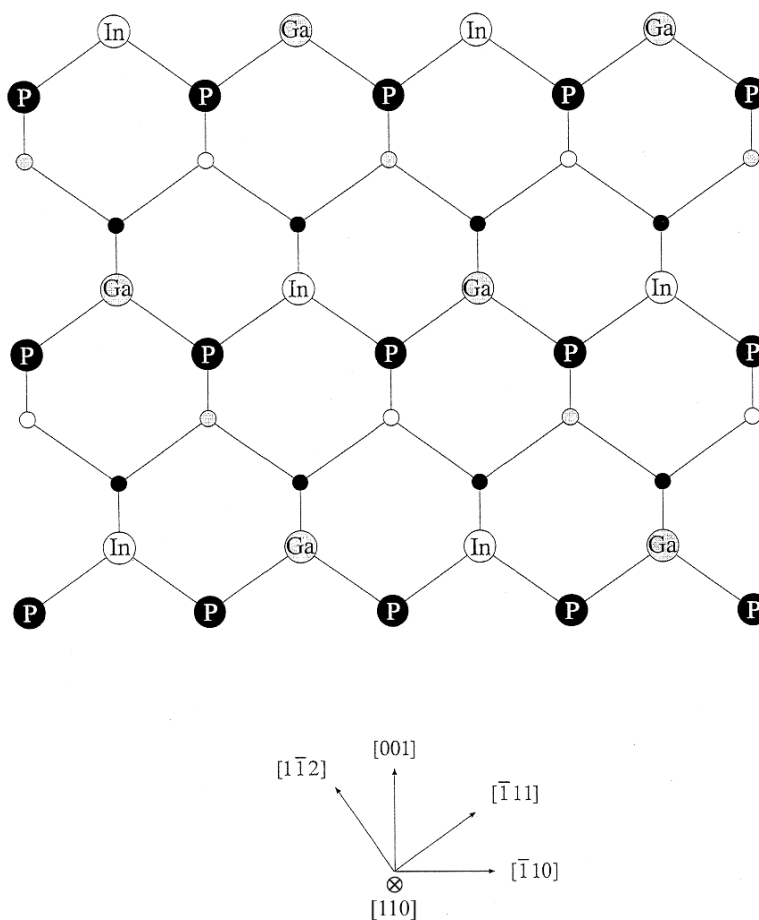


Figure 9. The (110) cleavage plane of ideally CuPt_B ordered single variant GaInP. Alternating In and Ga planes with ordering vector $[-111]$ intersect the (110) surface along $[1-12]$ directions.

$(\text{InP})_2(\text{GaP})_1[100]$ and of long period modulations in the electronic contrast $[101]$.

In cross-sectional STM it is possible to examine the interior atomic structure of ordered epitaxial layers grown on (001)-orientated substrates by cleaving the sample in ultra-high vacuum, thereby exposing a (110) crystal plane in cross section, and subsequently positioning the STM tip over the area of interest. The (111)_B ordering plane associated with CuPt_B ordering is normal to the (110) cleavage face and exposes alternating $[112]$ -like rows of Ga or In cations at the surface as shown in Fig.9. STM will discriminate

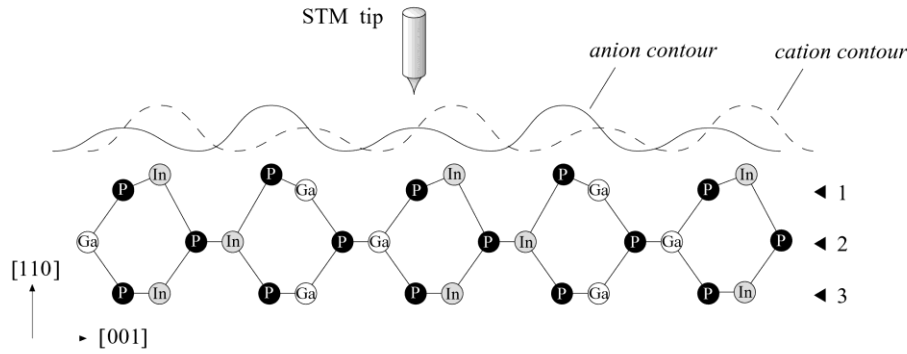


Figure 10. (110) STM contours for CuPtB order.

between the two types of surface cations in ordered semiconductor alloys on the basis of their different back bond lengths. Because an In to P back bond is approximately 0.2 \AA longer than the Ga to P bond, the In atoms will lie above the surface plane defined by the Ga atoms and thus appear brighter in the STM images as shown in Fig.10. The resulting schematic STM is shown in Fig.11, in plan view, with alternating [112]-like rows of In and Ga atoms stacked along the [-111] ordering direction. Anion discrimination in filled state images can also be used to image the pattern of cation sublattice ordering on a plane one layer below the cleavage plane due to the two different types of P atoms; those bonded to Ga or In subsurface atoms. Again, bond length differences cause P atoms bonded to subsurface Ga to extend from the cleavage plane and thus appear brighter than P bonded to subsurface In. The schematic STM image of the anion sublattice therefore looks no different than one of the cation sublattice.

In addition to detecting the presence of CuPt ordering in semiconductor alloys, more importantly, cross-sectional STM is capable of providing quantitative information on the degree of order in non-ideal samples through use of the pair correlation function:

$$g_{ideal}^{(2)}(R) = 4 \left\{ \frac{N_{In-Inpairs}^{ideal}(R)}{N_{cationpairs}(R)} \right\}, \quad (24)$$

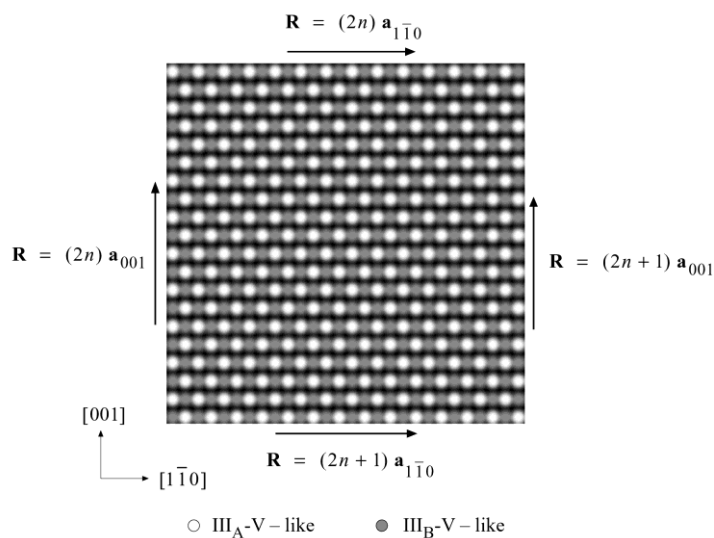


Figure 11. Schematic (110) STM image for CuPtB order.

where the term inside the brackets is the pair probability. This term has a value of $\frac{1}{2}$ for $\mathbf{R}=(2n)\mathbf{a}_{-110,001}$ and a value of 0 for $\mathbf{R}=(2n+1)\mathbf{a}_{-110,001}$, where \mathbf{a}_{-110} is a unit vector in the $[-110]$ direction, and n is an integer. The pair correlation function, g , provides a quantitative measure of the degree, range, and anisotropy of the spatial correlations between selected pairs of lattice sites by comparing the actual distribution of these sites, as a function of separation vector in the cleavage plane, \mathbf{R} , to a random distribution at the same density. In our case, this comparison amounts to normalizing the number of In-In pairs to the total number of cation pairs surveyed in such a way that a random distribution yields a pair correlation function whose value is one for all possible lattice vectors in the plane. In a random distribution only a quarter of the sites connected by a fixed separation vector yield In-In as opposed to In-Ga, or Ga-Ga pairs.

For the ideal case of or perfect order, this In-In pair probability, instead of being spatially uniform, oscillates between one-half and zero in both the $[-110]$ and $[001]$ directions, depending upon whether the corresponding lattice vector is an even or odd multiple of the appropriate primitive translation vector, \mathbf{a} . As a consequence of our normalization, the ideal pair correlation function oscillates between zero and two. The Bragg-Williams long-range order parameter, S , has a value of one for a perfectly ordered alloy, whereas $S = 0$ corresponds to a random alloy. For partially ordered alloys, S lies between zero and one. The oscillatory behaviour in the pair correlation function first identified with perfect order remains, but the magnitude of the deviation from unity is now identified with the square of S .

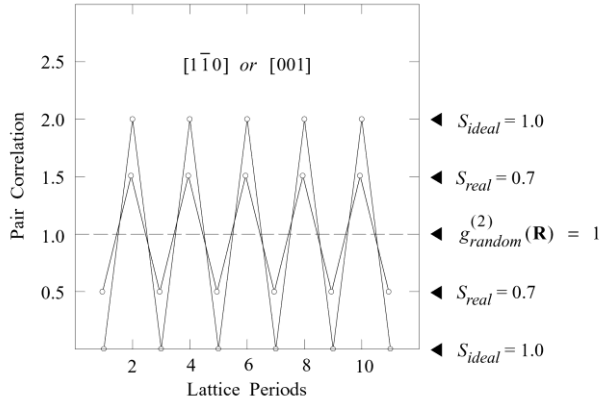


Figure 12. Schematic STM pair correlation for CuPtB order showing cases for no ordering, $S_{real}=0.7$, and $S_{ideal}=1.0$.

A schematic plot of the In-In pair correlation function versus separation for ideal CuPt order, together with the corresponding results for a random alloy and a case with $S = 0.7$ is shown in Fig.12. In the realistic case of finite sampling of populations in limited-area STM images, there will be uncertainties associated with statistical error. This will limit the ability to distinguish between long-range order and short-range order. However, if $S(\mathbf{R})$ remains independent of \mathbf{R} to within statistical uncertainty up to the largest separation vectors available, one can improve the cross-sectional STM estimate of the order parameter by considering the observations at each distinct lattice vector as independent measurements that may be properly averaged together.

Weimer et al[102] have used cross-sectional STM to investigate ordering and determine the local order parameter in GaInP and GaInAs grown by low-pressure metal organic chemical vapor deposition. Triethylgallium, trimethylindium, phosphine and arsine were used as precursors. The GaInP was grown on p-type (001) GaAs with a miscut of $4^\circ[111]$ -B, at 670°C , V/III ratio of 260 and growth rate of 5 \AA/s . The GaInAs layer was grown on p-type (001) InP with a miscut of $6^\circ[111]$ -B, at 550°C , V/III ratio of 240 and growth rate of 3.3 \AA/s . The samples were grown lattice-matched to their respective substrates. These conditions lead to reasonably strong ordering as confirmed by Raman and photoluminescence.

Fig.13 presents an atomic resolution view of the anion sublattice of the GaInP on GaAs interface obtained with a (110) cleave of the GaInP sample. The GaAs buffer layer is the homogeneous region in the lower right portion of the image, and the GaInP alloy film is the more complex looking region

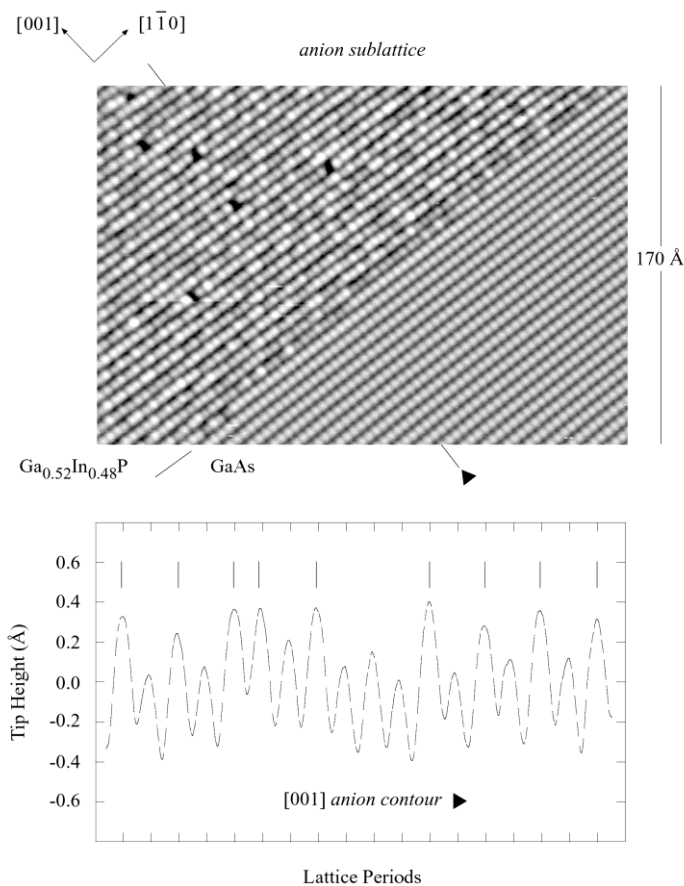


Figure 13. IIIA - IIIB site discrimination at the GaInP on GaAs interface.

here on the upper left. Three successive $[-111]-B$ steps are clearly resolved at the alloy/buffer interface, and a number of phosphorous vacancies appear within the alloy film. From this image and others we find that the $[-111]-B$ inclination is 4.1° from (001), in good agreement with the 4° miscut specified for this substrate. The sensitivity of distinguishing between phosphorous atoms back bonded to indium atoms and those back bonded to gallium atoms is illustrated in the surface section through the image, along the (001) growth direction, starting within a few lattice periods of the GaAs buffer and moving outward. Tick marks indicate those anion sites one can clearly identify with underlying indium atoms. The pattern is recognizably regular with the distinction between high and low corresponding to about 0.2 \AA . There are of course, occasional defects in the expected ordering pattern, e.g. where two In sites are adjacent to each other.

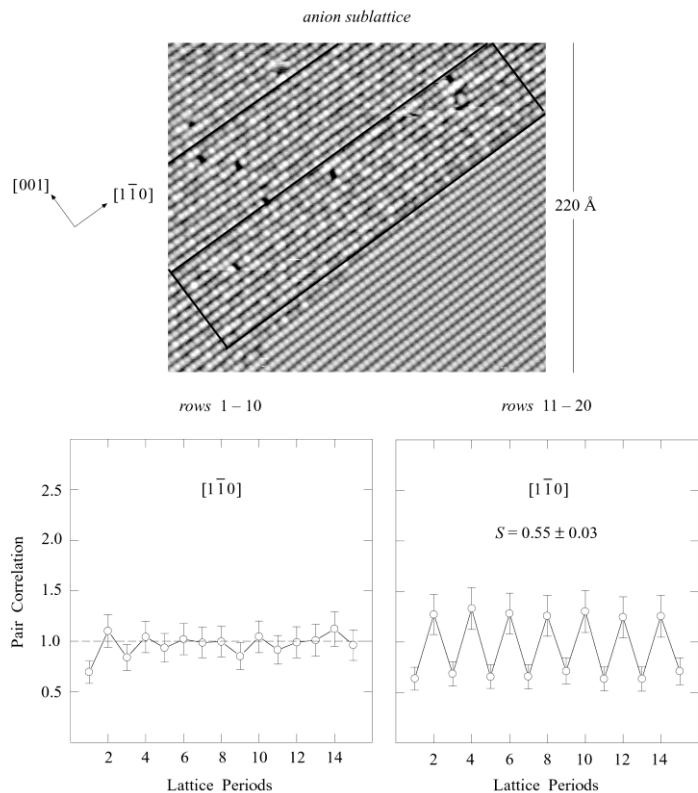


Figure 14. [001] evolution of the local order parameter.

The development of local order can be measured by following the evolution of the In-In pair correlation function, and hence the order parameter, during vapor phase epitaxy by exploring its behavior as a function of distance from the GaAs buffer. If one looks exclusively at the first 20 monolayers of the alloy film, as outlined by the black box closest to the substrate interface in Fig.14, one can see the faint emergence of short range order by observing several small amplitude oscillations in the pair correlation function shown in the plot labeled rows 1-10, that quickly decay toward a random distribution within a few [110] lattice periods. It is important to point out that this dramatic reduction in the behavior of the order parameter does not appear to be due to a local change in stoichiometry, because the In fraction detected with STM agrees, within statistical error, with the overall stoichiometry of the alloy determined from x-ray rocking curves. The evolution in the In-In pair correlation function over the next 20 monolayers, shown in the plot labeled rows 11-20, is similar to the behavior

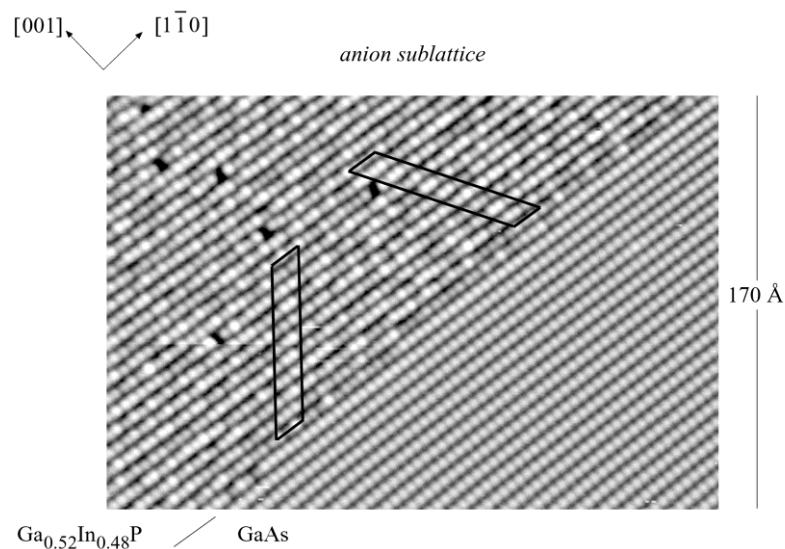


Figure 15. Atomically-abrupt antiphase boundaries near the GaInP – GaAs interface.

seen deeper into the alloy with the magnitude of the oscillations in $g(2)$ approaching a similar value. The ability to extract the local order parameter from STM pair correlation function demonstrates that the ordering process takes 10-20 monolayers to develop. This kind of detailed structural information on the atomic scale development of ordering is unattainable from commonly used optical (i.e. PL, PLE) or structural (e.g. TEM, x-ray) characterization techniques and illustrates the power of cross-sectional STM.

With STM we can also correlate the development of ordering with the step morphology of the interface and the defect structure of the alloy film within regions over which the order parameter is developing. In Fig.15, we have outlined a very interesting ordering defect, just above a step in the GaAs buffer layer, where we see two, adjacent $[1\bar{1}2]$ like rows of phosphorous anions back bonded to indium atoms that interrupt the expected checkerboard pattern. This structure suggests the presence of an antiphase boundary aligned with the $[1\bar{1}1]$ plane, as illustrated in the conventionally oriented schematic STM image shown below the experimental one. The actual structure is not a perfect match, with two gallium-like instead of indium-like sites in the third row, and another gallium for indium substitution further up, but this is to be expected with less than perfect order. There is also the suggestion of a second, complimentary antiphase boundary, aligned with the $[\bar{1}11]$ plane that appears in (110) cross-section as the mirror image of the first. These ordering defects represent either a local slip

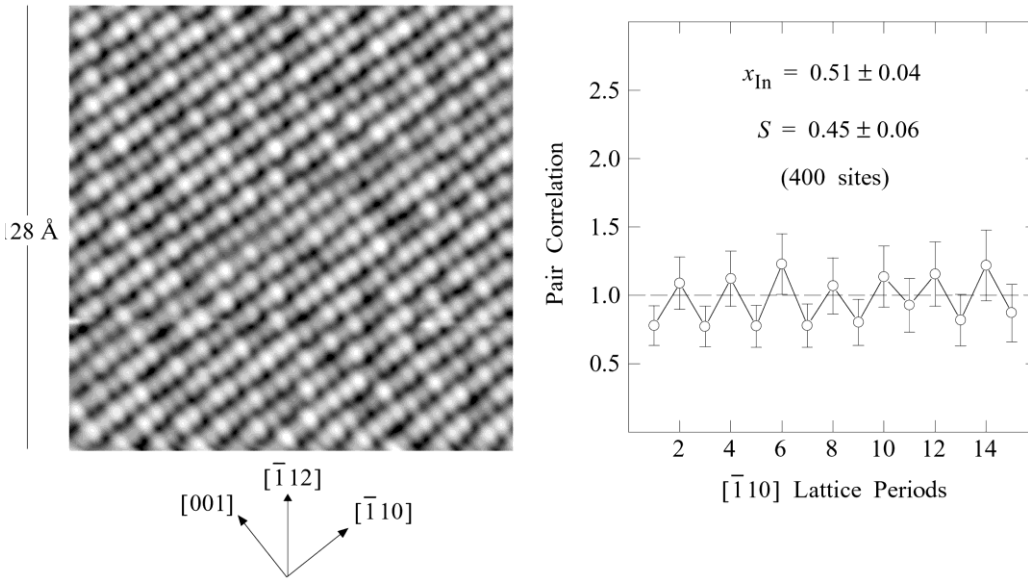


Figure 16. (001) STM image of ordered GaInAs and the $[-110]$ pair correlation.

along the cation ordering planes (defect on left) or a stacking fault in the cation ordering sequence, (defect on right).

Cross-sectional STM has also been used to investigate ordering in GaInAs grown on (001) InP substrates miscut 6° towards the $[111]_B$ direction. An example of a (110) STM image of a portion of an ordered GaInAs epilayer is shown in Fig. 16, along with the pair correlation analysis. One can easily recognize that the $[-112]$ and $[1-12]$ rows of indium atoms and the indium mole fraction detected with STM agree, within error, with the lattice-matched stoichiometry of 53%. Even though the number of sites sampled is relatively small (400 sites) in this case, the pair correlation function nevertheless oscillates in the expected way yielding an order parameter of $S = 0.45 \pm 0.06$. This value is somewhat higher than the value of 0.27 determined quantitatively on this sample by high-resolution x-ray diffraction measurements [103] of the superstructure peaks associated with $[111]$ CuPt ordering. This difference may be related to the problem of averaging over domains of different size, orientational variant, and degree of order in different variants in such a macroscopic measurement.

Cross-sectional STM can clearly add to the understanding of spontaneous ordering in semiconductor alloys through IIIa-IIIb site discrimination on the atomic-scale. The same techniques may be straightforwardly extended to single variant identification on a nanometer scale. The concept of a local order parameter naturally emerges from a statistical analysis of the STM

images based on the IIIa-IIIb pair correlation function and these ideas have been illustrated with a brief examination of the spatial evolution of the order parameter in the vicinity of the alloy/buffer interface. From the evidence for two types of atomically-abrupt antiphase boundaries presented in the cross-sectional STM signatures it is clear that the interfaces between ordered domains can be quite successfully probed using this technique.

7. STATISTICAL ASPECTS OF SPONTANEOUS ORDERING

A great deal of experimental and theoretical studies on spontaneous ordering have focused on the dependence of the ensemble average properties of the alloy on the order parameter: e.g., the band-gap reduction, valence band splitting, and optical anisotropy, as has been discussed in previous sections. In contrast, a fundamental aspect of spontaneous ordering relating to the statistical nature of the phenomenon has largely been ignored. Only until very recently, the most anticipated statistical effect of ordering, a reduction of alloy fluctuations, has been observed experimentally by Zhang et al[104] through a continuous reduction of the exciton linewidth with increasing order parameter. The statistical effects referred to here are those intrinsic to ordering and not related to imperfections in sample growth. For example, phenomena associated with the macroscopic spatial variations of the alloy composition, the order parameter, and antiphase domain boundaries[45,105-107] are considered to be related to growth imperfections which can in principle be eliminated or minimized by improving the growth technique. Evidently, the investigation of statistical effects for partially ordered structures is more difficult in terms of sample quality (experimentally) or computation effort (theoretically) than that of ensemble average properties. It is well known that the influence of alloy statistical fluctuations on many physical properties is a function of the alloy composition x . The first order effect can frequently be described by a simple function $x(1-x)$. For a spontaneously ordered alloy, the effects of alloy fluctuations will not only be a function of the average composition x but also of the order parameter η . Two statistical aspects of the influence of ordering are particularly interesting. One is the effect of alloy fluctuations on the band structure parameters (band gap and etc.), and the other is the effect on the crystal structural parameters (bond length etc.).

The first study of the statistical effect on the band structure was performed by Capaz and Koiller[25]. In their study the band gap fluctuation, obtained by averaging over 400 configurations of a 64 atom unit cell, was

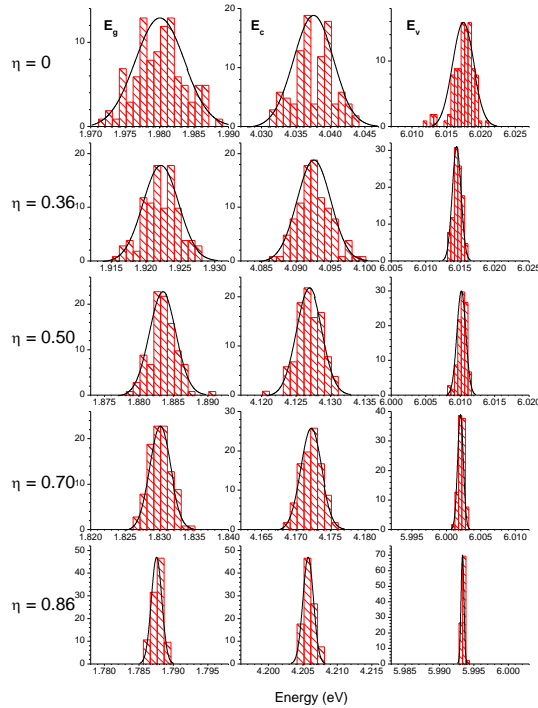


Figure 17. Histogram plots of the energy distributions of the band gap (E_g), conduction band edge (E_c) and valence band edge (E_v) for partially ordered $\text{Ga}_{0.5}\text{In}_{0.5}\text{P}$ alloys with order parameter $\eta = 0, 0.36, 0.50, 0.70,$ and 0.86 (from Ref.[107] of Zhang et al).

found to decrease on increasing the order parameter. A very recent study by Zhang et al[108] has attempted to simulate the partially ordered structure more realistically by using a rather large unit cell of ~ 3500 atoms and averaging over 100 configurations. The energy fluctuation not only for the band gap but also for the band edge of the conduction and valence band have been calculated. Fig.17 shows the histogram plots for these energy fluctuations, and Fig.18 shows the full width at half maximum (FWHM) of the histogram plots with a comparison of the experimentally measured excitonic linewidth[104]. The information for the band gap fluctuation is most relevant for various optical measurements (e.g., emission and absorption), but that for the individual band edge is most valuable for transport measurements related to either electrons or holes. In comparison with the results of Ref.[25], the new results indicate a somewhat stronger dependence of the alloy fluctuation on order parameter. Fig.17 also reveals that the band gap fluctuation does not obey the simple η^2 rule, although it

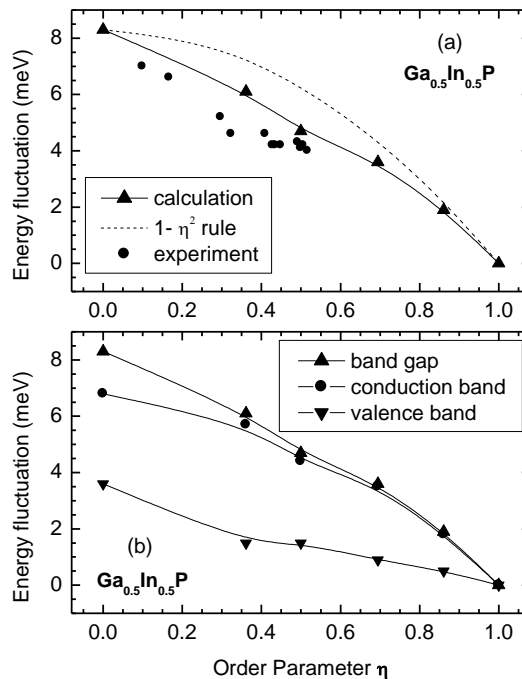


Figure 18. The energy fluctuation of the band gap $W_{\text{gap}}(\eta)$, of the conduction band edge $W_c(\eta)$, and of the valence band edge $W_v(\eta)$ for a partially ordered $\text{Ga}_{0.5}\text{In}_{0.5}\text{P}$ alloy, measured by the full width at half maximums (FWHM) of the histogram plots (shown in Fig.17), as a function of the order parameter η . (a) A comparison of the calculated $W_{\text{gap}}(\eta)$ with the low temperature photoluminescence linewidth $W_{\text{ex}}(\eta)$ of Ref.85 and a curve predicted by a simple η^2 dependence. (b) Calculated $W_c(\eta)$, $W_v(\eta)$ as well as $W_{\text{gap}}(\eta)$ (from Ref.[107] of Zhang et al).

was argued in Ref.[23] that the majority of physical properties should follow this rule.

As regards the effect of ordering on the crystal structure parameters, Capaz and Koiller[25] pointed out that if all the Ga-P and In-P bonds are divided into four groups: Ga-P and In-P bonds along the ordering direction (“O”) and in the lateral direction (“L”), the average bond length for each group would follow a η^2 dependence. However, a recent x-ray absorption fine-structure (XAFS) study by Meyer et al[109] on a partially ordered GaInP sample only resolved a single average Ga-P or In-P bond length for the entire sample (except for possible bond length modifications in certain localized regions), in agreement with the typical bimodal behavior of conventional alloys[110,111]. Zhang et al[108] pointed out that there are two factors which have prevented the observation of the ordering effect in

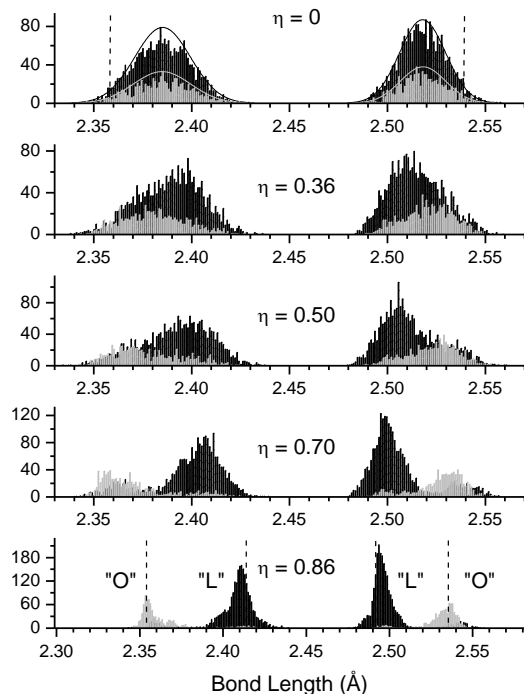


Figure 19. Histogram plots of the bond length distributions of partially ordered $\text{Ga}_{0.5}\text{In}_{0.5}\text{P}$ alloys with order parameter $\eta = 0, 0.36, 0.50, 0.70,$ and 0.86 . Black – for the “L” type bonds along the lateral directions; Gray - for the “O” type bonds along the ordering direction. The dashed vertical lines denote the Ga-P and In-P bond length in the binaries on the $\eta = 0$ panel (the up most), and in the fully order structure ($\eta = 1$) on the $\eta = 0.86$ panel (the bottom) (from Ref.[107] of Zhang et al).

the XAFS measurement: (1) the unpolarized nature of the measurement could not distinguish the O- and L-type bonds, and (2) the order parameter for the sample investigated was too small. Fig.19 shows the evolution of the distribution of the Ga-P and In-P bonds in partially ordered GaInP with order parameter. Fig.20 shows the average bond lengths and their statistical fluctuations as functions of η^2 . In agreement with the results of Ref.[25], the average bond length follows the η^2 dependence very well. One can see that (1) from Fig.20(a) for η up to 0.5, the “O” –“L” splitting is smaller than 0.2 Å which is the typical experimental uncertainty of any EXAFS measurements[109-111]; (2) the strong overlap between the distributions of O- and L-bonds and the 1: 3 ratio for the numbers of the types of bonds make it unfeasible to distinguish them by using any unpolarized EXAFS techniques, unless the sample is very highly ordered. Note that a superposition of the distribution of the O- and L-bond will result in a mixed

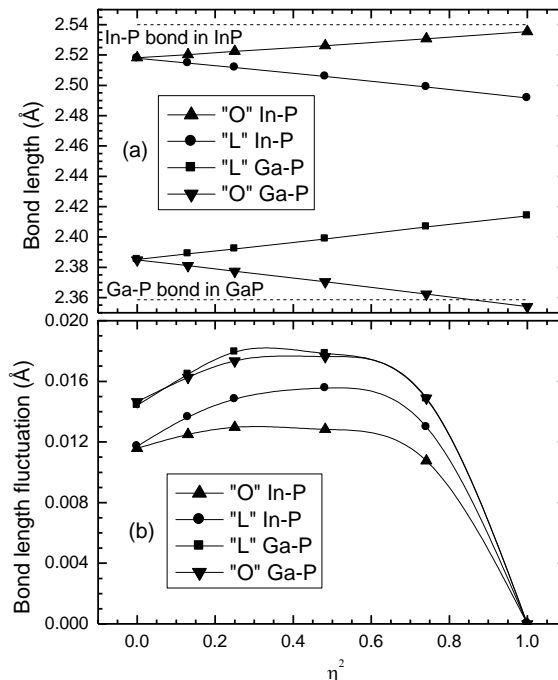


Figure 20. (a) Average bond lengths for the four types of bonds in partially ordered $\text{Ga}_{0.5}\text{In}_{0.5}\text{P}$ alloys versus η^2 ("O" – along the ordering direction, "L" – along the lateral directions). (b) Bond length fluctuations versus η^2 for the four types of bonds (from Ref.[107] of Zhang et al).

distribution that shows two peaks. An unpolarized XAFS measurement in principle should be able to resolve two average bond lengths for a highly ordered sample, but the average bond lengths so obtained will not follow the η^2 rule.

8. BAND OFFSET BETWEEN ORDERED GaInP AND GaAs

The GaInP/GaAs heterojunction bipolar transistor has emerged as a frontrunner for high-speed power transistors used for cellular communications. Because of the very practical device interest, the band alignment for the $\text{Ga}_x\text{In}_{1-x}\text{P}$ ($x \sim 0.5$)/GaAs heterostructure has attracted great deal of attention. A number of different approaches have yielded largely scattered values for the conduction band offset $\Delta E_c = E_c(\text{GaInP}) - E_c(\text{GaAs})$,

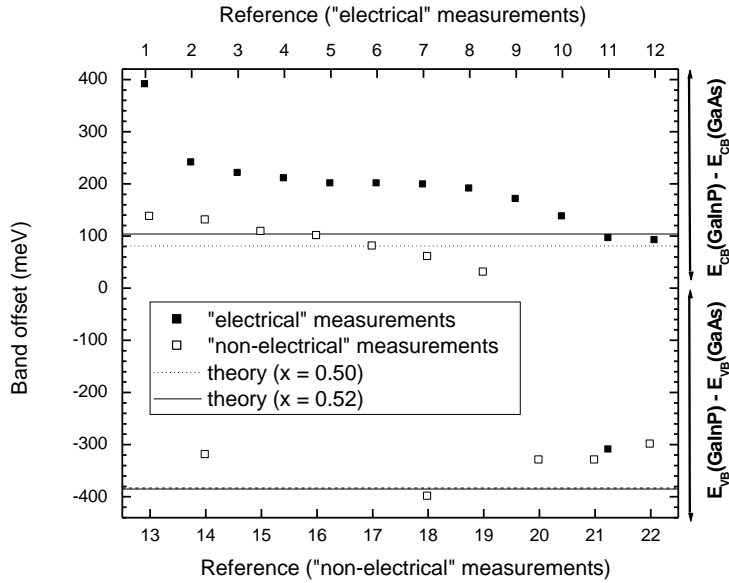


Figure 21. Comparison between the calculated values of Ref.[141] and experimental data for the conduction and valence band offset. Tick labels 1-22 correspond to the reference numbers 112-133 (from Ref.[141] of Zhang et al).

ranging from 30 to 390 meV[112-133]. It has recently been noticed that the existence of spontaneous ordering in the GaInP layer could significantly alter the band offset[124,134-138]. It thus appears that besides the possible intrinsic limitation of each technique[112-133], the ordering effect has contributed to the large scatter in the reported values at least to some extent. The scatter for theoretically calculated values is actually smaller. For the random-GaInP/GaAs heterostructure, Harrison found $\Delta E_c = 160$ meV[139]; Foulon et al found a valence band offset $\Delta E_v = 320$ to 390 meV[140]; Froyen et al found $\Delta E_c = 120$ meV and $\Delta E_v = 370$ meV[141]. A most recent calculation of Zhang et al gave $\Delta E_c = 81$ (104) meV and $\Delta E_v = 383$ (385) meV for $x = 0.50$ (0.52)[27,142]. Fig.21 shows the values of ΔE_c and/or ΔE_v for the GaInP/GaAs heterostructure found in the literature. It appears that the conduction band offsets derived from various “electrical measurements” (e.g., capacitance-voltage, current-voltage) [112-125] show a larger scatter (ranging from 390 to 91 meV) as compared to those obtained from other techniques: 108 ± 6 meV from internal photoemission[126], 137 meV or 100 meV from BEEM spectroscopy[124,127], 80 meV from photoluminescence[128], 160 meV[139], 120 meV[141], and 104 meV ($x = 0.52$) or 81 meV ($x = 0.50$)[142] from theoretical calculations. Note that for the conduction band offset the results of the more recent “electrical”

measurements (Refs.[121-123]), except for Ref.[117], have approached those of “non-electrical” measurements (Refs.[124-129]) and the theoretical results.

The conduction band offset between ordered-GaInP and GaAs has also been a critical issue on the debate of the mechanism for the up-converted PL observed in GaInP/GaAs heterostructure[136,143-145]. Up-converted PL for an ordered-GaInP/GaAs heterostructure was first reported by Driessen[143]. He observed PL from the GaInP layer for excitation at the GaAs band gap, and explained the phenomenon by the so-called cold Auger process[143]. Su et al later attributed the same phenomenon to a two-step two-photon absorption (TS-TPA) process[136]. Driessen subsequently showed that the up-conversion could even be observed for (AlGa)InP/GaAs interfaces[144]. Since the band offset was likely to increase significantly with the incorporation of Al, they believed that the two-step model of Su et al was invalid. However, this later result of Driessen et al actually only proved that the nearly zero band offset was not a necessity for the up-conversion, and did not exclude the possible role of the two-step mechanism in the observed up-conversion at the ordered-GaInP/GaAs interface. Kita et al performed a time-resolved up-conversion study on the ordered-GaInP/GaAs interface[145]. They pointed out that there were two channels for the up-conversion: (1) direct TS-TPA processes for both electrons and holes localized near the interface; and (2) TS-TPA and Auger processes caused by the GaAs PL, but they excluded the need of a flat conduction band alignment (since they believed that the sample should have a type I alignment). Although based on the existing data it is inconclusive as to what is the dominant mechanism for the up-conversion and whether the band offset is the single dominant factor for generating the up-conversion, an accurate knowledge of how the band offset changes with the ordering is important for answering these questions. Froyen et al’s calculation indicated that the conduction band alignment between GaAs and perfectly CuPt ordered GaInP would become type II with $\Delta E_c = -130$ meV, but that the valence band alignment would remain type I with a reduced value of $\Delta E_v = 270$ meV. Applying the η^2 rule to the band edge energies, Froyen et al obtained a crossover point at $\eta_0 = 0.70$, implying that all the samples used for the up-conversion studies were most likely in the type I region[35]. However, a recent band structure calculation by Zhang et al[27] has shown that the η^2 rule is generally invalid. Thus, a direct calculation of the band edge energy with varying order parameter is highly desirable. Fig.22 shows the results of the first such attempt, where the band offsets are given both as a function of the order parameter and band gap[142]. According to Fig. 22,

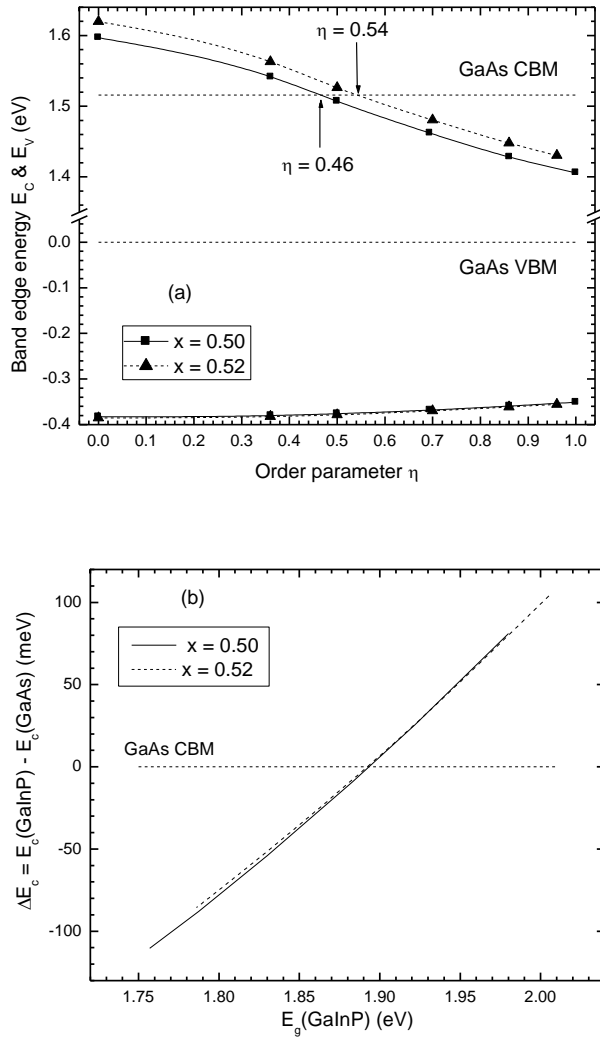


Figure 22. Band edge energies of partially CuPt ordered $\text{Ga}_x\text{In}_{1-x}\text{P}$ alloys, varying with (a) order parameter η and (b) band gap E_g (from Ref.[141] of Zhang et al).

the crossover point is $\eta_0 = 0.54$ for $x = 0.52$. Therefore, on one hand, for the sample used by Kita et al[145] with $E_g \sim 1.89$ eV, the order parameter actually should have been very close to η_0 instead of $\eta = 0.44$ as estimated by the authors, implying that a nearly flat conduction band alignment could have played a role in the observed up-conversion. On the other hand, in order to justify the existence of a type II band alignment, Kwork et al[146] claimed that their sample had a value of η as high as 0.75 to conform with

the crossover point $\eta_0 = 0.7$ estimated by Froyen et al[141]. Since the PL peak was taken as a measure of the band gap and the η^2 rule was used for converting the “band gap reduction” to the order parameter, Kwok et al likely overestimated the order parameter for their sample. Zeman et al[137,138] found that a set of ordered-GaInP/GaAs samples that exhibited the up-conversion had ΔE_c in a range of ± 3 meV and PL peak energies around 1.9 eV. If one takes the PL peak as a measure of band gap, one finds that Zeman et al’s results agree quite well with that of Fig.22. However, one has to keep in mind two factors: (1) a PL peak is frequently not an accurate measure of the band gap; (2) the samples they used were grown on exact (001) substrates, and thus, were not expected to have the simple CuPt ordered structure, but rather to have the double variant structure[65-68]. Also, we notice that the result of Ref.[130] (i.e., $\Delta E_c = 30$ meV for an ordered GaInP sample with 60 meV band gap reduction) appears to agree quite well with the theoretical result of Ref.[142], as shown in Fig.22. We would like to point out that the finding of Ref.[117], $\Delta E_c = 200$ meV not changing with ordering, is contradictory with either the experimental data of Refs.[134-138] or the theoretical results of Refs.[141,142].

9. NOVEL SUPERLATTICES–ORIENTATIONAL SUPERLATTICES

It is well-known that when an exact (001) substrate or $[111]_A$ tilt substrate is used, two $[111]_B$ CuPt ordered variants are usually present simultaneously. However, the domain size, the stacking direction as well as the regularity of the domain distribution strongly depends on the growth conditions (e.g., the exact substrate tilt angle and orientation, growth rate, epilayer thickness and etc.)[67,68]. Quasi-periodic structures of domain twins of the two ordered variants have been observed either along the [001] growth direction[63,64,68] or along the $[\bar{1}10]$ direction[147] (where we define the $[\bar{1}11]$ and $[1\bar{1}1]$ as the ordering direction for the two variants). The [001] structures are found to have a periodicity of typically less than 5 nm, as observed in the TEM study (e.g., Morita et al[63], Baxter et al[64], Ahrenkiel et al[68]) and recently in a x-ray study by Li et al[36]. The $[\bar{1}10]$ structures usually have a large periodicity of the order of 1 μm and show facets on the sample surface, as reported by Friedman et al[147]. Ahrenkiel found that during growth the double variant structure gradually evolved from the [001] stacking (roughly below 2 μm thickness) to the $[\bar{1}10]$ stacking arrangement for the upper part of the epilayer for film thickness up to 10 μm [148]. In fact, domain twin structure is a frequently seen phenomenon

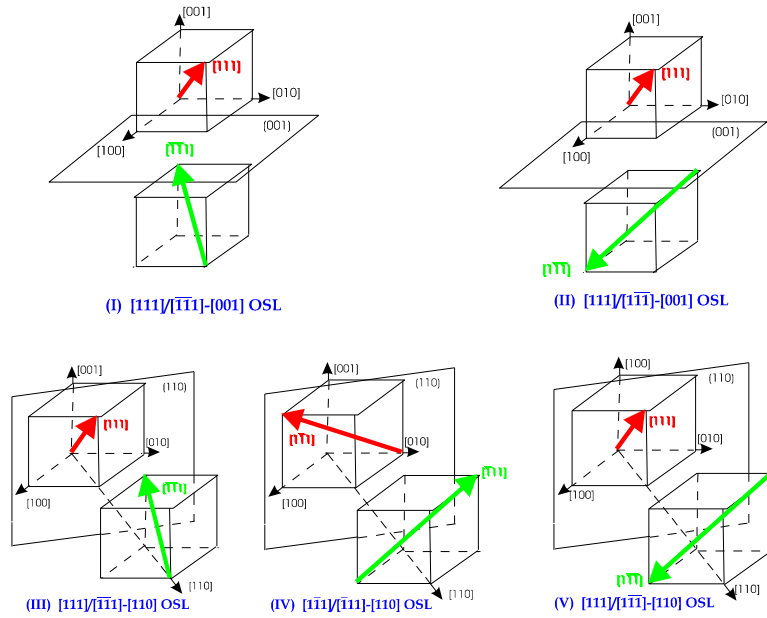


Figure 23. Five polytype orientational superlattices based on CuPt-ordered GaInP alloys (from Ref.[65] of Mascarenhas et al).

in different kinds of crystals, but typically the domain size is of the order of the wavelength of light or bigger. Thus, when viewed under polarized light, one expects to see bright and dark contrast between domains. In deed, optical effects have been observed in ordered GaInP with the large $[\bar{1}10]$ type double variant structure by Alsina et al[149] and Sapriel and Hassine[150]. However, quantum mechanical effects which are expected to occur when the domain size is reduced to less than a few hundred Å have only been discussed recently, first by Ikonic et al[151] for a hypothetical twinning superlattice formed by periodically stacked $[111]$ twin defects in diamond and zinc-blende type semiconductors, and then by Mascarenhas et al[65,66] for orientational superlattices (OSLs) formed by domain twins of CuPt ordered III-V alloys. What distinguishes the OSL from the conventional superlattice where the superlattice effect results from a discontinuity in the band edge energy (a scalar) ips that the superlattice effect for the OSL originates from a discontinuity (a rotation) in the orientation of the symmetry axis (a vector) for the constituent layers. Fig.23 schematically depicts five simple polytypes which can be formed by two ordered variants, where polytype I, III, and IV can be viewed as comprised of twin boundaries of two $[111]_A$ or $[111]_B$ ordered domains, and polytype II and V as comprised of twin boundaries f a $[111]_A$ and a $[111]_B$ ordered

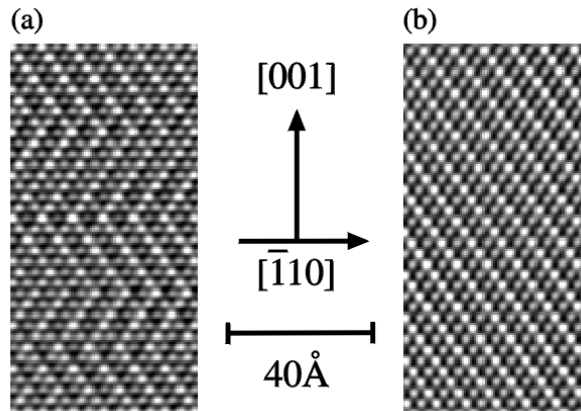


Figure 24. High-resolution cross-sectional TEM pictures of (a) a double-variant ordered and (b) a single-variant ordered GaInP alloys (from Ref. [68] of Zhang et al).

domain. Since the ordering induced phase transition is ferroelastic[65], Sapriel and Hassine[150] have shown that only polytype I, III and IV are strain-compatible (for free standing CuPt ordered layers).

As demonstrated by Zhang et al[67,68,152], the CuPt ordered micro-domain twin structures that closely resemble the proposed OSL have distinctly different electronic and optical properties from those of the single variant CuPt ordered structure. Fig.24 shows a comparison of high resolution TEM pictures of an OSL like sample and a simple CuPt ordered sample[68]. Fig.25 shows polarized PL and PLE spectra for a pair of ordered samples both having order parameters near $\eta = 0.50$ [152]: one grown on a 6°B tilted substrate, and thus, a typical single variant ordered sample; whilst the other grown on a 6°A tilted substrate, and thus having an OSL like structure along the $[001]$ direction. As is evident that the second sample not only has a 60 meV larger band gap than the first one but also shows much stronger optical anisotropy between the $[110]$ and $[\bar{1}10]$ polarizations. The enhanced optical anisotropy can be readily explained by the symmetry change for the topmost valence band state upon the formation of an OSL[68], and was the first observed signature of the OSL effect[66]. One might attempt to ascribe the band gap increase for the double variant ordered sample shown in Fig.25 as being due to a lower degree of order, but the enhanced optical anisotropy cannot possibly be explained by this effect. To further rule out this possibility, the order parameter as well as the structural parameters of each individual variant have been determined experimentally[36]. In addition, Fig.26 further reveals that the correlation between the band gap reduction and valence band splitting are clearly different for the single and double variant order samples[67].

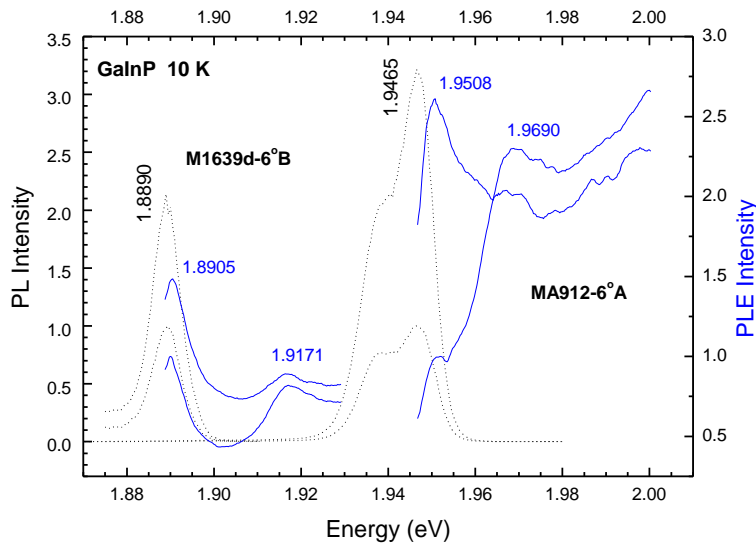


Figure 25. A comparison of polarized PL and PLE spectra between a single-variant CuPt ordered and a double-variant CuPt ordered GaInP with the same measured order parameter (from Ref.[151] of Zhang et al).

Mascarenhas et al[65,66] first attempted to model the band structure of OSLs using a 6-band \mathbf{k},\mathbf{p} envelope function approach. They showed that even without band offsets and effective mass discontinuities, the OSL was capable of giving rise to quantum confinement effects that are normally achieved via the band offsets in conventional superlattices. The optical anisotropy due to the symmetry change of the wavefunction is associated with the “orientational” nature of this superlattice, and this becomes the dominant effect, because the confinement energy for the hole (the downward shift of the valence band edge) is relatively small. A comparison with a later first principle calculation of Wei and Zunger[153] indicates that the simple envelope function can indeed describe the valence band very well[66]. However, the first principle calculations of both Munzar et al (where the authors referred to the ordered domain twins as antiphase domain boundaries or APBs)[154] and Wei and Zunger[153] revealed a larger shift in the conduction band edge than that of the valence band. Even though both the domain size and the order parameter for the double variant ordered sample can now be determined experimentally[36], a quantitative comparison with theory is still impossible, because the full band structure calculation has

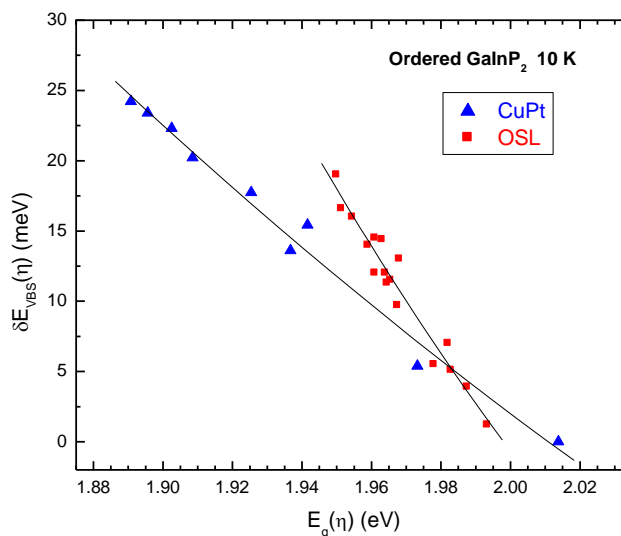


Figure 26. A comparison of the functional dependence of the valence-band splitting versus the band-gap between single-variant and double-variant (small domain) ordered GaInP₂ samples (from Ref.[67] of Zhang et al).

only been performed for the fully ordered structure with small number of layers[153,154].

10. EXTRINSIC EFFECTS IN ORDERED GaInP

For CuPt ordered GaInP samples used in the early stage of the ordering study, it was plausible that there existed considerable structural non-uniformity, which was evidenced by the observed relatively large PL linewidth (typically > 10 meV for partially ordered samples[16,39,45,155,156], compared to < 7 meV for disordered samples[104,155]. Although these of samples were useful for the purpose of demonstrating some important effects of ordering (e.g., the ordering features in TEM, the band gap reduction, the optical anisotropy), they also gave rise to certain peculiar properties which attracted a great deal of attention for a period of time as though these properties were inherent to ordering. The so-called “moving emission”[156] has been perhaps the most extensively discussed issue among these extrinsic phenomena observed in ordered GaInP alloys. A broad PL band, either as the only major emission band for some samples[155] or the lower energy band for samples having two PL bands[156], was found to shift to high energy with increasing

excitation density at a rate (> 10 meV/decade) significantly faster than that for the band edge emission of a typical semiconductor alloy, or for the typical donor-acceptor pair emission. DeLong et al[156] attributed this moving emission, which exhibited a long decay time > 1 μ s, to a spatially indirect transition between the disordered and ordered domain, and suggested that the ordered domains were distributed throughout a disordered matrix. However, Hahn et al[157] shown later, by means of stereo images, that domain boundaries were microscopically thin, and the reason that they generally appeared as broad dark lines in TEM dark-field images was due to their projection onto the image plane. This study supports the conclusion based on spectroscopy studies that there is no disordered phase surrounding ordered domains, because not has only no optical transition associated with the disordered phase ever been observed for partially ordered samples[29-31] but also the spatial variation of the order parameter has been found to be minimal in the sub-micron scale[105]. DeLong et al[158] also observed that the moving emission only appeared in double-variant ordered samples, thus, suggesting that the moving emission was related to the interfaces between domains with different ordering directions. Ernst et al[159,160] investigated the correlation between optical properties and the ordered domain size. They found that samples with small domain sizes typically showed a single broad PL peak (as in the case of Ref.[155]), while samples with large domain sizes typically showed two PL peaks of which the higher energy peak (HE) was due to the band edge excitonic transition and the lower energy peak (LE) behaved similarly to the “moving emission” of Ref.[156]. However, the two peaks in Ref.[159] were well separated under low excitation density (the separation is larger than 30 meV, see Fig.5 for typical spectra of a sample of this type) and considerably sharper than those observed in the earlier study of Ref.[156]. Since the large domain samples used by Ernst et al were grown on substrates tilted 6° toward the $[111]_B$ direction, thus, being single-variant ordered, the correlation made by DeLong et al[158] between the “moving emission” and the double-variant ordering appears not to be valid in general. Indeed, in Ref. [158], samples on 6°_B tilted substrates did not show the “moving peak”; instead, a peak, behaving like a normal impurity transition, appeared at ~ 20 meV below the band edge transition. Similar spectra to those reported by DeLong et al have also been reported for single-variant samples grown under similar conditions (e.g., Ref.[47] and Ref.[72]). Thus, the “moving emission” does not always appear with partial ordering, and the below band gap emission could have different origins for different samples. Given these factors, any attempt to provide a generalized model or theory for the extrinsic below band gap emission is unrealistic.

There have been quite a few efforts to investigate the below band gap emission in partially ordered GaInP by using sub-micron spatially resolved

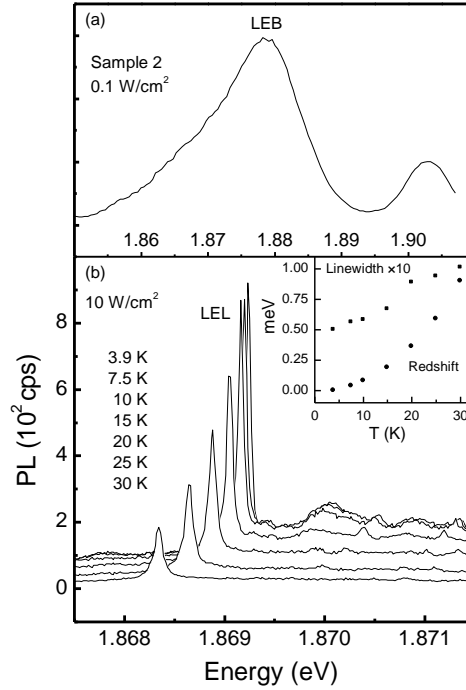


Figure 27. (a) Macro PL spectra cw excited at 1.908 eV. (b) Micro PL from the apertured sample area at lattice temperatures from 3.9 K (largest) to 30 K (smallest). Curves are plotted on the same origin, i.e., not displaced. Inset: the linewidth and peak position relative to the 3.9 K peak are plotted as a function of temperature (from Ref.[161] of Fluegel et al).

PL and PLE[105-107,161,162]. Gregor et al[161] reported an anti-correlation for the intensity of the band edge and the below band gap emission, thus drawing a conclusion that the HE and LE emission originated from distinct spatial locations, and indicated that their results supported the interpretation of the LE emission being spatially indirect. Although Smith et al[106] also observed the anti-correlation for the PL intensities, they found that the LE emission coexisted with the HE emission in regions whose scales were much larger than the average domain size of 0.9 μm , which contradicts the idea that the LE emission originates solely from domain boundaries of either the ordered/disordered or antiphase domains, and suggests that other defects within the ordered domain might also contribute to the LE emission. Although the LE emission has been shown to contain some sharp emission lines in several studies by Cheong et al[105], Smith et al[[106], and Kops et al[107], only Kops et al have attempted to correlated them to a specific type

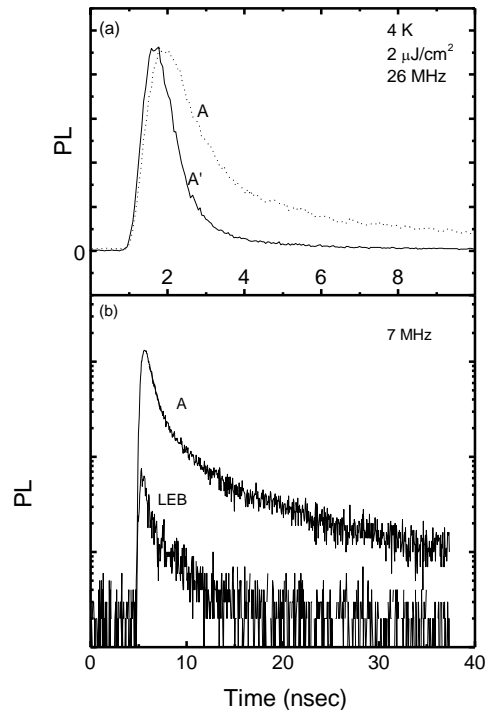


Figure 28. (a) Normalized time-resolved PL at two LEL peaks (A and A' for a single exciton and a multi-exciton state, respectively). (b) Log plot of the PL decay at the ground state peak and at the LE band (from Ref.[161] of Fluegel et al).

of crystalline defect, namely, antiphase domain boundaries (APBs). Kops et al investigated the LE emission in partially ordered samples with different order parameters by varying temperature, external magnetic field, and excitation density. They indicated that the LE emission could be decomposed into two distinctly different types of transitions: a broad emission band (LEB) and superimposed sharp emission lines (LEL) (with a width of 0.3 – 1.0 meV). LEB and LEL were found to have different temperature and magnetic field dependence: the linewidth of the LEB showed a large temperature broadening while that of the LEL was temperature independent within an accuracy of $\pm 0.1\text{meV}$; the LEL showed an excitonic behavior under magnetic field while the LEB's behavior was typical of free carriers (similar to the behavior of the moving peak observed in macro-PL by Jones et al[73]). While the origin for the LEB was not explicitly discussed except that the LEB might be related to a recombination between a strongly localized electron and a free hole, Kops et al associated

the LEL to disks at APBs of two monolayers of InP aligned in the $[111]_B$ direction, and pointed out a correlation between the number of the LELs and the density of APBs as shown in TEM pictures. In an effort to give a unified picture for the LE below band gap emission, Matilla et al[163] performed an empirical pseudopotential calculation for the electronic states of the APB suggested by Kops et al, and claimed that their results explained the experimentally observed type II behavior for the below band gap emission. The calculation indicated that that for the APB with two adjacent InP layers (the so-called V_2 structure) the first hole state (h_1) would be localized at the interface, whereas the higher hole states (h_2 and etc.) and electron states (e_1 and etc.) would be delocalized in the bulk CuPt ordered region. Matilla et al assigned the indirect $e_1 - h_1$ transition to the LE emission, but it was not clear which of the LEB or LEL they meant. If they meant the LEB, they actually disagreed with Kops et al who believed that the LEB was related to a strongly localized electron state rather than a localized hole state; if they meant the LEL, the sharp emission line and the excitonic behavior under magnetic field seem to disprove this transition being type II. Not only has no long lifetime ever been measured for the LEL, but it was also shown by Smith et al[106] that the sharp lines could appear even within an ordered domain. Besides these points, we would like to point out that the specific kind of APB's suggested by Kops et al and modeled by Matilla et al have not been clearly observed in any microscopic study, although it has been found that the APB's may exist with almost any orientations[64,107,160]. Thus, even though this particular type of APB could perhaps generate a hole bound state, there is no direct experimental evidence for relating the theoretical results to the experimentally observed LEB or LEL. However, it is clear that the LEL are related to some type of defects in partially ordered alloys, but the exact nature of these defects is yet unknown.

The data of Kops et al[107] indicated that the behavior of LEL was much like that of quantum dots (QDs). However, unlike those QDs which normally distribute in a two dimensional plane (either by "self-assembling"[164] or formed unintentionally due to lateral layer width fluctuations in a quantum well[165]), these defects may be view as three dimensionally distributed QDs and thus LELs resemble the recombination of bound excitons associated with impurities in a bulk crystal[166]. One could in fact consider a single impurity analogous to a smallest QD. Using a higher spectral resolution than that of Kops et al, Fluegel et al[162] have resolved LELs with linewidth as small as 50 μeV (still limited by the spectral resolution), and found that the LEL linewidth increased by a factor of two on increasing the temperature to 30 K, just like the temperature dependence of the linewidth for the impurity transition[166]. They also observed that the transition energy decreased with increasing temperature, which merely

reflects the band structure change of the host semiconductor with temperature. The results are shown in Fig.27. Through time resolved measurements, it has now been revealed that for a LEL due either to a single exciton or to a multi-exciton bound state, the radiative decay time is of the order of ~ 1 ns, typical of a direct transition. Even the LEB has been found to have a decay time similar to that of the LEL. Fig.28 shows typical PL decay curves for the LELs (one for a single exciton state and one for a multiexciton state) and the LEB. Another interesting finding is that by performing selective excitation at individual LEL's, an energy transfer process amongst different LEL's has been demonstrated, which again shows a closed similarity between the LEL's in ordered GaInP and impurity bound excitons in a bulk semiconductor. For instance, this type of energy transfer has long been observed amongst different nitrogen related trap centers in GaP:N[167].

11. CONCLUSIONS

There has been significant progress made during the past two decades in understanding and controlling the phenomenon of spontaneous ordering during epitaxial growth of semiconductor alloys. A variety of experimental techniques have been successfully utilized for probing the structural and electronic changes that result from this phenomenon and there now appears to be reasonable agreement between some of the experimental and theoretical results. However, even for the GaInP system there still remains a great deal of work to be done with respect to clarifying the ordering mechanism, obtaining higher order parameters, elucidating the effect of spontaneously generated electric fields on the properties of the ordered GaInP/GaAs heterojunction and understanding the role played by the microstructure on some of the peculiar optical properties. The more interesting research on the effects of statistical fluctuations that are tunable by control of the order parameter has only just begun and the studies that have been discussed should provide a solid foundation for further advances in the field.

12. ACKNOWLEDGEMENT

We would like to acknowledge the invaluable contributions of Brian Fluegel, Steve Smith, Hyeonsik M. Cheong, S. Phil Ahrenkiel, Andrew Norman, M. Al-Jassim, Jerry Olson, John Geisz, D. Friedman, Mark Hanna, Michael Kozhevnikov, Venky Narayanamuti, Lin-Wang Wang, Sveree

Froyen, Eric D. Jones, Rebecca Forrest, Jianhua Li, Simon Moss, Jeremy Steinschneider, and Michael Weimer to the research presented in this chapter. We thank the Office of Science/Basic Energy Sciences/Division of Materials Sciences for their generous support of this research at NREL.

REFERENCES

- ¹ I. J. Murgatroyd, A. G. Norman, G. R. Booker, and T. M. Kerr, *J. Electron Microsc.* **35**, 1497 (1986).
- ² A. G. Norman, D. Phil. Thesis, University of Oxford, 1987.
- ³ I. J. Murgatroyd, D. Phil. Thesis, University of Oxford, 1987.
- ⁴ A. G. Norman, R. E. Mallard, I. J. Murgatroyd, G. R. Booker, A. H. Moore, and M. D. Scott, *TED, TEM and HREM studies of atomic ordering in AlInAs (x~0.5) epitaxial layers grown by organometallic vapour epitaxy*, in *Proc. Microsc. Semicond. Mater. Conf., Oxford, 6–8 April 1987 (IOP Conf. Ser. No. 87)*, edited by A. C. Cullis and P. D. Augustus (IOP Publishing, Bristol, UK, 1987), pp. 77.
- ⁵ R. Hull, K. W. Carey, J. E. Fouquet, G. A. Reid, S. J. Rosner, D. Bimberg, and D. Oertel, in *GaAs and Related Compounds 1986* (Inst. of Phys., Bristol, 1987), Vol. 83, pp. 209.
- ⁶ M. A. Shahid, S. Mahajan, D. E. Laughlin, and H. M. Cox, *Phys. Rev. Lett.* **58**, 2567 (1987).
- ⁷ Y.-E. Ihm, N. Otsuka, J. Klem, and H. Morkoc, *Appl. Phys. Lett.* **51**, 2013 (1987).
- ⁸ O. Ueda, M. Takikawa, J. Komeno, and I. Umebu, *Jpn. J. Appl. Phys.* **26**, L1824 (1987).
- ⁹ A. Gomyo, T. Suzuki, and S. Iijima, *Phys. Rev. Lett.* **60**, 2645 (1988).
- ¹⁰ J. P. Goral, M. M. Al-Jassim, J. M. Olson, and A. Kibbler, in *Epitaxy of Semiconductor Layered Structures* (1988), Vol. 102, pp. 583.
- ¹¹ S. McKernan, B. C. D. Cooman, C. B. Carter, D. P. Bour, and J. R. Shealy, *J. Mater. Res.* **3**, 406 (1988).
- ¹² P. Bellon, J. P. Chevalier, G. P. Martin, E. Dupont-Nivet, C. Thiebaut, and J. P. André, *Appl. Phys. Lett.* **52**, 567 (1988).
- ¹³ M. Kondow, H. Kakibayashi, and S. Minagawa, *J. Cryst. Growth* **88**, 291 (1988).
- ¹⁴ A. N. Pikhtin, *Sov. Phys. Semicond.* **11**, 245.
- ¹⁵ T. Suzuki, A. Gomyo, S. Iijima, K. Kobayashi, S. Kawata, I. Hino, and T. Yuasa, *Jpn. J. Appl. Phys.* **27**, 2098 (1988).
- ¹⁶ A. Gomyo, K. Kobayashi, S. Kawata, I. Hino, T. Suzuki, and T. Yuasa, *J. Cryst. Growth* **77**, 367 (1986).
- ¹⁷ Y. Ohba, M. Ishikawa, H. Sugawara, M. Yamamoto, and T. Nakanishi, *J. Cryst. Growth* **77**, 374 (1986).
- ¹⁸ S. R. Kurtz, J. M. Olson, and A. Kibbler, *Solar Cells* **24**, 307 (1988).
- ¹⁹ A. Mascarenhas, S. R. Kurtz, A. Kibbler, and J. M. Olson, *Phys. Rev. Lett.* **63**, 2108 (1989).
- ²⁰ S.-H. Wei and A. Zunger, *Phys. Rev. B* **39**, 3279 (1989).
- ²¹ T. Kurimoto and N. Hamada, *Phys. Rev. B* **40**, 3889 (1989).
- ²² S.-H. Wei, L. G. Ferreira, J. E. Bernard, and A. Zunger, *Phys. Rev. B* **42**, 9622 (1990).
- ²³ D. B. Laks, S.-H. Wei, and A. Zunger, *Phys. Rev. Lett.* **69**, 3766 (1992).
- ²⁴ S.-H. Wei, D. B. Laks, and A. Zunger, *Appl. Phys. Lett.* **62**, 1937 (1993).
- ²⁵ R. B. Capaz and B. Koiller, *Phys. Rev. B* **47**, R4044 (1993).
- ²⁶ K. A. Mäder and A. Zunger, *Phys. Rev. B* **51**, 10462 (1995).
- ²⁷ Y. Zhang, A. Mascarenhas, and L.-W. Wang, *Phys. Rev. B* **63**, R201312 (2001).

- ²⁸ Y. Zhang and A. Mascarenhas, *Phys. Rev. B* **51**, 13162 (1995).
- ²⁹ R. G. Alonso, A. Mascarenhas, G. S. Horner, K. A. Bertness, S. R. Kurtz, and J. M. Olson, *Phys. Rev. B* **48**, 11833 (1993).
- ³⁰ P. Ernst, C. Geng, F. Scholz, H. Schweizer, Y. Zhang, and A. Mascarenhas, *Appl. Phys. Lett.* **67**, 2347 (1995).
- ³¹ B. Fluegel, Y. Zhang, H. M. Cheong, A. Mascarenhas, J. F. Geisz, J. M. Olson, and A. Duda, *Phys. Rev. B* **55**, 13647 (1997).
- ³² S.-H. Wei and A. Zunger, *Phys. Rev. B* **57**, 8983 (1998).
- ³³ R. Tycko, G. Dabbagh, S. R. Kurtz, and J. P. Goral, *Phys. Rev. B* **45**, 13452 (1992).
- ³⁴ D. Mao, P. C. Tylor, S. R. Kurtz, M. C. Wu, and W. A. Harrison, *Phys. Rev. Lett.* **76**, 4769 (1996).
- ³⁵ R. L. Forrest, T. D. Golding, S. C. Moss, Y. Zhang, J. F. Geisz, J. M. Olson, A. Mascarenhas, E. Ernst, and C. Geng, *Phys. Rev. B* **58**, 15 355 (1998).
- ³⁶ J. H. Li, J. Kulik, V. Holy, Z. Zhong, S. C. Moss, Y. Zhang, S. P. Ahrenkiel, A. Mascarenhas, and J. Bai, *Phys. Rev. B* **63**, 155310 (2001).
- ³⁷ S.-H. Wei and A. Zunger, *J. Chem. Phys.* **107**, 1931 (1997).
- ³⁸ T. Kanata, M. Nishimoto, H. Nakayama, and T. Nishino, *Phys. Rev. B* **45**, 6637 (1992).
- ³⁹ D. J. Mowbray, R. A. Hogg, M. S. Skolnick, M. C. DeLong, S. R. Kurtz, and J. M. Olson, *Phys. Rev. B* **46**, 7232 (1992).
- ⁴⁰ T. Kanata, M. Nishimoto, H. Nakayama, and T. Nishino, *Appl. Phys. Lett.* **63**, 512 (1993).
- ⁴¹ J. J. Hopfield, *J. Phys. Chem. Solids* **15**, 97 (1960).
- ⁴² J. L. Shay, E. Buehler, and J. H. Wernick, *Phys. Rev. B* **3**, 2004 (1971).
- ⁴³ S.-H. Wei and A. Zunger, *Appl. Phys. Lett.* **56**, 662 (1990).
- ⁴⁴ D. Teng, J. Shen, K. E. Newman, and B.-L. Gu, *J. Phys. Chem. Solids* **52**, 1109 (1991).
- ⁴⁵ G. S. Horner, A. Mascarenhas, S. Froyen, R. G. Alonso, K. Bertness, and J. M. Olson, *Phys. Rev. B* **47**, 4041 (1993).
- ⁴⁶ G. S. Horner, A. Mascarenhas, R. G. Alonso, D. J. Friedman, K. Sinha, K. A. Bertness, J. G. Zhu, and J. M. Olson, *Phys. Rev. B* **48**, 4944 (1993).
- ⁴⁷ H. M. Cheong, Y. Zhang, A. Mascarenhas, J. F. Geisz, and J. M. Olson, *J. Appl. Phys.* **83**, 1773 (1998).
- ⁴⁸ J. S. Luo, J. M. Olson, K. A. Bertness, M. E. Raikh, and T. E. V., *J. Vac. Sci. Technol. B* **12**, 2552 (1994).
- ⁴⁹ E. Greger, K. H. Gulden, M. Moser, G. Schmiedel, P. Kiesel, and G. H. Dohler, *Appl. Phys. Lett.* **70**, 1459 (1997).
- ⁵⁰ T. Kita, A. Fujiwara, H. Nakayama, and T. Nishino, *Appl. Phys. Lett.* **66**, 1794 (1995).
- ⁵¹ F. Alsina, M. Garriga, M. I. Alonso, J. Pascual, J. Camassel, and R. W. Glew, in *Proceedings of the 22nd International Conference in Physics of Semiconductors*, edited by D. J. Lockwood (World Scientific, Singapore, 1995), pp. 253.
- ⁵² B. Fluegel, A. Mascarenhas, J. F. Geisz, and J. M. Olson, *Phys. Rev. B* **57**, R6787 (1998).
- ⁵³ M. Moser, R. Winterhoff, C. Geng, I. Queisser, F. Scholz, and A. Dornen, *Appl. Phys. Lett.* **64**, 235 (1994).
- ⁵⁴ R. Wirth, A. Moritz, C. Geng, F. Scholz, and A. Hangleiter, *Phys. Rev. B* **55**, 1730 (1997).
- ⁵⁵ Y. Zhang, B. Fluegel, A. Mascarenhas, J. F. Geisz, J. M. Olson, F. Alsina, and A. Duda, *Solid State Commun.* **104**, 577 (1997).
- ⁵⁶ G. G. Forstmann, F. Barth, H. Schweizer, M. Moser, C. Geng, F. Scholz, and E. P. O'Reilly, *Semicond. Sci. Technol.* **9**, 1268 (1994).
- ⁵⁷ E. Greger, K. H. Gulden, P. Riel, H. P. Schweizer, M. Moser, G. Schmiedel, P. Kiesel, and G. H. Dohler, *Appl. Phys. Lett.* **68**, 2383 (1996).
- ⁵⁸ E. Greger, K. H. Gulden, P. Riel, M. Moser, T. Kippenberg, and G. H. Dohler, *Appl. Phys. Lett.* **71**, 3245 (1997).

- ⁵⁹ G. L. Bir and G. E. Pikus, *Symmetry and Strain-Induced Effects in Semiconductors* (Wiley, New York, 1974).
- ⁶⁰ S.-H. Wei and A. Zunger, Phys. Rev. B **49**, 14337 (1994).
- ⁶¹ Y. Zhang, A. Mascarenhas, P. Ernst, F. A. J. M. Driessen, D. J. Friedman, K. A. Bertness, J. M. Olson, C. Geng, F. Scholz, and H. Schweizer, J. Appl. Phys. **81**, 6365 (1997).
- ⁶² E. G. Tsitsishvili, Phys. Rev. B **59**, 10044 (1999).
- ⁶³ E. Morita, M. Ikeda, O. Kumagai, and K. Kaneko, Appl. Phys. Lett. **53**, 2164 (1988).
- ⁶⁴ C. S. Baxter, W. M. Stobbs, and J. H. Wilkie, Journal of Crystal Growth **112**, 373 (1991).
- ⁶⁵ A. Mascarenhas, Y. Zhang, R. G. Alonso, and S. Froyen, Solid State Commun. **100**, 47 (1996).
- ⁶⁶ Y. Zhang and A. Mascarenhas, Phys. Rev. B **56**, 9975 (1997).[Erratum, Phys. Rev. B **56**, 9975 (1997).].
- ⁶⁷ Y. Zhang, A. Mascarenhas, S. P. Ahrenkiel, D. J. Friedman, J. Geisz, and J. M. Olson, Solid State Commun. **109**, 99 (1998).
- ⁶⁸ Y. Zhang, B. Fluegel, S. P. Ahrenkiel, D. J. Friedman, J. F. Geisz, J. M. Olson, and A. Mascarenhas, Mat. Res. Soc. Symp. Proc. **583**, 255 (2000).
- ⁶⁹ M. I. Dyakonov and V. I. Perel, *Theory of optical spin orientation of electrons and nuclei in semiconductors*, in *Optical Orientation*, edited by F. Meier and B. P. Zakharchenya (North-Holland, Amsterdam, 1984), pp. 11.
- ⁷⁰ F. Ciccacci, E. Molinari, and N. E. Christensen, Solid State Commun. **62**, 1 (1987).
- ⁷¹ T. Kita, M. Sakurai, K. Bhattacharya, K. Yamashita, T. Nishino, C. Geng, F. Scholz, and H. Schweizer, Phys. Rev. B **57**, R15044 (1998).
- ⁷² B. Fluegel, Y. Zhang, A. Mascarenhas, J. F. Geisz, J. M. Olson, and A. Duda, Phys. Rev. B **60**, R11261 (1999).
- ⁷³ E. D. Jones, D. M. Follstaedt, S. K. Lyo, and J. R. P. Schneider, Mat. Res. Soc. Symp. Proc. **281**, 61 (1993).
- ⁷⁴ P. Emanuelsson, M. Drechsler, D. M. Hofmann, B. K. Meyer, M. Moser, and F. Scholz, Appl. Phys. Lett. **64**, 2849 (1994).
- ⁷⁵ M. E. Raikh and E. V. Tsiper, Phys. Rev. B **49**, 2509 (1994).
- ⁷⁶ A. Franceschetti, S.-H. Wei, and A. Zunger, Phys. Rev. B **53**, 13992 (1995).
- ⁷⁷ Y. C. Yeo, M. F. Li, T. C. Chong, and P. Y. Yu, Phys. Rev. B **55**, 16414 (1997).
- ⁷⁸ P. Ernst, Y. Zhang, F. A. J. M. Driessen, A. Mascarenhas, E. D. Jones, C. Geng, F. Scholz, and H. Schweizer, J. Appl. Phys. **81**, 2814 (1997).
- ⁷⁹ Y. Zhang, A. Mascarenhas, and E. D. Jones, J. Appl. Phys. **83**, 448 (1998).
- ⁸⁰ D. E. Aspnes, J. P. Harbison, A. A. Studna, and L. T. Florez, J. Vac. Sci. Technol A **6**, 1327 (1988).
- ⁸¹ J. S. Luo, J. M. Olson, S. R. Kurtz, D. J. Arent, K. A. Bertness, M. E. Raikh, and E. V. Tsiper, Phys. Rev. B **51**, 7603 (1995).
- ⁸² B. A. Philips, I. Kamiya, K. Hingerl, L. T. Florez, D. E. Aspnes, S. Mahajan, and J. P. Harbison, Phys. Rev. Lett. **74**, 3640 (1995).
- ⁸³ J. Callaway, *Quantum Theory of the Solid State* (Academic Press, Boston, 1991).
- ⁸⁴ S. H. Wei and A. Zunger, Phys. Rev. B **51**, 14110 (1995).
- ⁸⁵ J. S. Luo, J. M. Olson, Y. Zhang, and A. Mascarenhas, Phys. Rev. B **55**, 16385 (1997).
- ⁸⁶ M. Zorn, P. Kurpas, A. I. Shkrebtii, B. Junno, A. Bhattacharya, K. Knorr, M. Weyers, L. Samuelson, J. T. Zettler, and W. Richter, Phys. Rev. B **60**, 8185 (1999).
- ⁸⁷ S. B. Zhang, S. Froyen, and A. Zunger, Appl. Phys. Lett. **67**, 3141 (1995).
- ⁸⁸ H. Murata, I. H. Ho, T. C. Hsu, and G. B. Stringfellow, Appl. Phys. Lett. **67**, 3747 (1995).
- ⁸⁹ H. Murata, I. H. Ho, L. C. Su, Y. Hosokawa, and G. B. Stringfellow, J. Appl. Phys. **79**, 6895 (1996).
- ⁹⁰ H. W. M. Salemink and O. Albrektsen, Phys. Rev. B **47**, 16044 (1993).

- ⁹¹ K.-J. Chao, C.-K. Shih, D. W. Gotthold, and B. G. Streetman, *Phys. Rev. Lett* **79**, 16044 (1997).
- ⁹² J. F. Zheng, J. D. Walker, M. B. Salmeron, and E. R. Weber, *Phys. Rev. Lett* **72**, 2414 (1994).
- ⁹³ M. Pfister, M. B. Johnson, S. F. Alvarado, H. W. M. Salemink, U. Marti, D. Martin, F. Morier-Genoud, and F. K. Reinhart, *Appl. Phys. Lett.* **67**, 1459 (1995).
- ⁹⁴ J. Harper, M. Weimer, D. Zhang, C.-H. Lin, and S. S. Pei, *J. Vac. Sci. Technol. B* **16**, 1389 (1998).
- ⁹⁵ H. Chen, R. M. Feenstra, P. G. Piva, R. D. Goldberg, I. V. Mitchell, G. C. Aers, P. J. Poole, and S. Charbonneau, *Appl. Phys. Lett.* **75**, 79 (1999).
- ⁹⁶ R. M. Feenstra, D. A. Collins, D. Z. Y. Ting, M. W. Wang, and T. C. McGill, *Phys. Rev. Lett* **72**, 2749 (1994).
- ⁹⁷ S. L. Skala, W. Wu, J. R. Tucker, J. W. Lyding, A. Seabaugh, E. A. B. III, and D. Jovanovic, *J. Vac. Sci. Technol. B* **13**, 660 (1995).
- ⁹⁸ A. Y. Lew, S. L. Zuo, E. T. Yu, and R. H. Miles, *Phys. Rev. B* **57**, 6534 (1998).
- ⁹⁹ J. Harper, M. Weimer, D. Zhang, C.-H. Lin, and S. S. Pei, *Appl. Phys. Lett.* **73**, 2805 (1998).
- ¹⁰⁰ N. Liu, C. K. Shih, J. Geisz, A. Mascarenhas, and J. M. Olson, *Appl. Phys. Lett.* **73**, 1979 (1998).
- ¹⁰¹ A. J. Heinrich, M. Wenderoth, M. A. Rosentreter, K. Engel, M. A. Schneider, R. G. Ulbrich, E. R. Weber, and K. Uchida, *Applied Physics A* **66**, S959 (1998).
- ¹⁰² M. Weimer, M. Hanna, and J. Steinschnider, unpublished.
- ¹⁰³ R. L. Forrest, E. D. Meserole, R. T. Nielsen, M. S. Goorsky, Y. Zhang, A. Mascarenhas, M. Hanna, and S. Francoeur, *Mat. Res. Soc. Symp. Proc.* **583**, 249 (2000).
- ¹⁰⁴ Y. Zhang, A. Mascarenhas, S. Smith, J. F. Geisz, J. M. Olson, and M. Hanna, *Phys. Rev. B* **61**, 9910 (2000).
- ¹⁰⁵ H. M. Cheong, A. Mascarenhas, J. F. Geisz, J. M. Olson, M. W. Keller, and J. R. Wendt, *Phys. Rev. B* **57**, R9400 (1998).
- ¹⁰⁶ S. Smith, H. M. Cheong, B. D. Fluegel, J. F. Geisz, J. M. Olson, L. L. Kazmerski, and A. Mascarenhas, *Appl. Phys. Lett.* **74**, 706 (1999).
- ¹⁰⁷ U. Kops, P. G. Blome, M. Wenderoth, R. G. Ulbrich, C. Geng, and F. Scholz, *Phys. Rev. B* **61**, 1992 (2000).
- ¹⁰⁸ Y. Zhang, A. Mascarenhas, and L.-W. Wang, *Phys. Rev. B* **64**, 125207 (2001).
- ¹⁰⁹ D. C. Meyer, K. Richter, P. Paufler, and G. Wagner, *Phys. Rev. B* **59**, 15253 (1999).
- ¹¹⁰ J. C. Mikkelsen(Jr.) and J. B. Boyce, *Phys. Rev. Lett.* **49**, 1412 (1982).
- ¹¹¹ J. B. Boyce and J. C. Mikkelsen(Jr.), *J. Cryst. Growth* **98**, 37 (1989).
- ¹¹² K. Kodama, M. Hoshino, K. Kilahara, M. Takikawa, and M. Ozeki, *Jap. J. Appl. Phys.* **25**, L127 (1986).
- ¹¹³ S. L. Feng, J. Krynicki, V. Donchev, J. C. Bourgoin, M. D. Forte-Poisson, C. Brylinski, S. Delage, H. Blanck, and S. Alaya, *Semicon. Sci. Technol.* **8**, 2092 (1993).
- ¹¹⁴ M. A. Rao, E. J. Caine, H. Kroemer, S. I. Long, and D. I. Babic, *J. Appl. Phys.* **61**, 643 (1987).
- ¹¹⁵ T. W. Lee, P. A. Houston, R. Kumar, X. F. Yang, G. Hill, M. Hopkinson, and P. A. Claxton, *Appl. Phys. Lett.* **60**, 474 (1992).
- ¹¹⁶ W. Liu, S. K. Fan, T. S. Kim, E. A. Beam, and D. B. Davito, *IEEE Electron Devices* **40**, 1378 (1993).
- ¹¹⁷ P. Krispin, M. Asghar, A. Knauer, and H. Kostial, *J. Cryst. Growth* **220**, 220 (2000).
- ¹¹⁸ D. Biswas, N. Debbar, P. Bhattacharya, M. Razeghi, M. Defour, and F. Omnes, *Appl. Phys. Lett.* **56**, 833 (1990).
- ¹¹⁹ M. O. Watanabe and Y. Ohba, *Appl. Phys. Lett.* **50**, 906 (1987).

- ¹²⁰ M. S. Faleh, J. Tasselli, J. P. Bailbe, and A. Marty, *Appl. Phys. Lett.* **69**, 1288 (1996).
- ¹²¹ S. Lan, C. Q. Yang, W. J. Wu, and H. D. Liu, *J. Appl. Phys.* **79**, 2162 (1996).
- ¹²² A. Lindell, M. Pessa, A. Salokatve, F. Bernardini, R. M. Nieminen, and M. Paalanen, *J. Appl. Phys.* **82**, 3374 (1997).
- ¹²³ Y.-H. Cho, K.-S. Kim, S.-W. Ryu, S.-K. Kim, B.-D. Choe, and H. Lim, *Appl. Phys. Lett.* **66**, 1785 (1995).
- ¹²⁴ J. J. O'Shea, C. M. Reaves, S. P. DenBaars, M. A. Chin, and V. Narayanamurti, *Appl. Phys. Lett.* **69**, 3022 (1996).
- ¹²⁵ G. Arnaud, P. Boring, B. Gil, J.-C. Garcia, J.-P. Landesman, and M. Leroux, *Phys. Rev. B* **46**, 1886 (1992).
- ¹²⁶ M. A. Haase, M. J. Hafich, and G. Y. Robinson, *Appl. Phys. Lett.* **58**, 616 (1981).
- ¹²⁷ M. Kozhevnikov, V. Narayanamurti, A. Mascarenhas, Y. Zhang, J. M. Olson, and D. L. Smith, *Appl. Phys. Lett.* **75**, 1128 (1999).
- ¹²⁸ K.-S. Kim, Y.-H. Cho, B.-D. Choe, W. G. Jeong, and H. Lim, *Appl. Phys. Lett.* **67**, 1718 (1995).
- ¹²⁹ J. Chen, J. R. Sites, I. L. Spain, M. J. Hafich, and J. Y. Robinson, *Appl. Phys. Lett.* **58**, 744 (1991).
- ¹³⁰ T. Kobayashi, K. Taira, F. Nakamura, and H. Kawai, *J. Appl. Phys.* **65**, 4898 (1989).
- ¹³¹ M. Leroux, M. L. Fille, B. Gil, J. P. Landesman, and J. C. Garcia, *Phys. Rev. B* **47**, 6465 (1993).
- ¹³² M. F. Whitaker, D. J. Dunstan, M. Missous, and L. Gonzalez, *Phys. Stat. Sol. B* **198**, 349 (1996).
- ¹³³ O. Dehaese, X. Wallart, O. Schuler, and F. Mollot, *J. Appl. Phys.* **84**, 2127 (1998).
- ¹³⁴ Q. Liu, S. Derksen, A. Lindner, F. Scheffer, W. Prost, and F.-J. Tegude, *J. Appl. Phys.* **77**, 1154 (1995).
- ¹³⁵ Q. Liu, S. Derksen, W. Prost, A. Lindner, and F.-J. Tegude, *J. Appl. Phys.* **79**, 305 (1996).
- ¹³⁶ Z. P. Su, K. L. Teo, P. Y. Yu, and K. Uchida, *Solid State Commun.* **99**, 933 (1996).
- ¹³⁷ J. Zeman, G. Martinez, P. Y. Yu, S. H. Kwok, and K. Uchida, *Phys. Stat. Sol. (b)* **211**, 239 (1999).
- ¹³⁸ J. Zeman, G. Martinez, P. Y. Yu, and K. Uchida, *Phys. Rev. B* **55**, R13 428 (1997).
- ¹³⁹ W. A. Harrison, *J. Vac. Sci. Technol. B* **1**, 126 (1983).
- ¹⁴⁰ Y. Foulon, C. Priester, G. Allan, J. C. Garcia, and J. P. Landesman, *J. Vac. Sci. Technol. B* **10**, 1754 (1992).
- ¹⁴¹ S. Froyen, A. Zunger, and A. Mascarenhas, *Appl. Phys. Lett.* **68**, 2852 (1996).
- ¹⁴² Y. Zhang, A. Mascarenhas, and L.-W. Wang, unpublished.
- ¹⁴³ F. A. J. M. Driessen, *Appl. Phys. Lett.* **67**, 2813 (1995).
- ¹⁴⁴ F. A. J. M. Driessen, H. M. Cheong, A. Mascarenhas, S. K. Deb, P. R. Hageman, G. J. Bauhuis, and L. J. Giling, *Phys. Rev. B* **54**, R5263 (1996).
- ¹⁴⁵ T. Kita, T. Nishino, C. Geng, F. Scholz, and H. Schweizer, *Phys. Rev. B* **59**, 15358 (1999).
- ¹⁴⁶ S. H. Kwok, P. Y. Yu, K. Uchida, and T. Arai, *Appl. Phys. Lett.* **71**, 1110 (1997).
- ¹⁴⁷ D. J. Friedman, G. S. Horner, S. R. Kurtz, K. A. Bertness, J. M. Olson, and J. Moreland, *Appl. Phys. Lett.* **65**, 878 (1994).
- ¹⁴⁸ S. P. Ahrenkiel, unpublished.
- ¹⁴⁹ F. Alsina, J. Pascual, M. Garriga, M. I. Alonso, S. Tortosa, C. Geng, F. Scholz, and R. W. Glew, *Solid State Commun.* **101**, 10 (1997).
- ¹⁵⁰ J. Sapriel and A. Hassine, *Phys. Rev. B* **56**, R7112 (1997).
- ¹⁵¹ Z. Ikonic, G. P. Srivastava, and C. J. Inkson, *Phys. Rev. B* **48**, 17181 (1993).
- ¹⁵² Y. Zhang and A. Mascarenhas, *J. Raman Spec.* **32**, 831 (2001).
- ¹⁵³ S.-H. Wei, S. B. Zhang, and A. Zunger, *Phys. Rev. B* **59**, R2478 (1998).

- ¹⁵⁴ D. Munzar, E. Dobrocka, I. Vavra, R. Kudela, M. Harvanka, and N. E. Christensen, *Phys. Rev. B* **57**, 4642 (1998).
- ¹⁵⁵ J. E. Fouquet, V. M. Robbins, S. J. Rosner, and O. Blum, *Appl. Phys. Lett.* **57**, 1566 (1990).
- ¹⁵⁶ M. C. DeLong, W. D. Ohlsen, I. Viohl, P. C. Taylor, and J. M. Olson, *J. Appl. Phys.* **70**, 2780 (1991).
- ¹⁵⁷ G. Hahn, C. Geng, P. Ernst, H. Schweizer, F. Scholz, and F. Phillipp, *Superlattices and Microstructures* **22**, 301 (1997).
- ¹⁵⁸ M. C. DeLong, C. E. Ingefield, P. C. Taylor, L. C. Su, I. H. Ho, T. C. Hsu, G. B. Stringfellow, K. A. Bertness, and J. M. Olson, in *Proc. 21th Int. Symp. Comp. Semicond.*, edited by H. Goronkin and U. Mishra (IOP Publishing, Bristol, 1995), pp. 207.
- ¹⁵⁹ P. Ernst, C. Geng, F. Scholz, and H. Schweizer, *Phys. Status Solidi B* **193**, 213 (1996).
- ¹⁶⁰ P. Ernst, C. Geng, G. Hahn, F. Scholz, H. Schweizer, F. Phillipp, and A. Mascarenhas, *J. Appl. Phys.* **79**, 2633 (1996).
- ¹⁶¹ M. J. Gregor, P. G. Blome, R. G. Ulbrich, P. Grossmann, S. Grosse, J. Feldmann, W. Stolz, E. O. Göbel, D. J. Arent, M. Bode, K. A. Bertness, and J. M. Olson, *Appl. Phys. Lett.* **67**, 3572 (1995).
- ¹⁶² B. Fluegel, S. Smith, Y. Zhang, A. Mascarenhas, J. F. Geisz, and J. M. Olson, unpublished.
- ¹⁶³ T. Matilla, S.-H. Wei, and A. Zunger, *Phys. Rev. Lett.* **83**, 2010 (1999).
- ¹⁶⁴ D. Leonard, M. Krishnamurthy, C. M. Reaves, S. P. Denbaars, and P. M. Petroff, *Appl. Phys. Lett.* **63**, 3203 (1993).
- ¹⁶⁵ A. Zrenner, L. V. Butov, M. Hagn, G. Abstreiter, G. Böhm, and G. Weimann, *Phys. Rev. Lett.* **72**, 3382 (1994).
- ¹⁶⁶ D. E. McCumber and M. D. Sturge, *J. Appl. Phys.* **34**, 1682 (1963).
- ¹⁶⁷ P. J. Wiesner, R. A. Street, and H. D. Wolf, *Phys. Rev. Lett.* **35**, 1366 (1975).